

Supporting information

A Pair of Enantiomeric Bis-*seco*-abietane Diterpenoid from *Cryptomeria fortunei*

Lu Feng,[†] Attila Mándi,[‡] Chunping Tang,^{†,§} Tibor Kurtán,[‡] Shuai Tang,^{||} Chang-Qiang Ke,^{†,§}
Ning Shen,^{||} Ge Lin,[§] Sheng Yao,^{*,†,§} and Yang Ye^{*,†,§,⊥}

[†] State Key Laboratory of Drug Research, and Natural Products Chemistry Department, and ^{||} Division of Antitumor Pharmacology, Shanghai Institute of Materia Medica, Chinese Academy of Sciences, Shanghai 201203, People's Republic of China

[‡] Department of Organic Chemistry, University of Debrecen, P. O. Box 400, H-4002 Debrecen, Hungary

[§] SIMM-CUHK Joint Research Laboratory for Promoting Globalization of Traditional Chinese Medicines, Shanghai 201203, People's Republic of China

[⊥] School of Life Science and Technology, ShanghaiTech University, Shanghai 201203, People's Republic of China

Contents

Experimental section

- 1.1 General Experimental Procedures
- 1.2 Plant Material
- 1.3 Extraction and Isolation
- 1.4 Characteristics of Compounds
- 1.5 X-ray Crystallographic Analysis
- 1.6 Chiral-phase Separation of **1**
- 1.7 Computational Methods for ECD of Compounds **1a**, **1b**
- 1.8 Enantiomeric Synthesis of **1a** and **1b**
- 1.9 Chiral-phase Analysis of Synthetic **1a** and **1b**

Figures

Figure S1. The chiral-phase HPLC chromatogram of **1**

Figure S2. Experimental ECD spectra of (+)-**1a** and (-)-**1b** in MeOH.

Figure S3. Experimental ECD spectrum of **1a** in MeOH (black) compared with the BH&HLYP/TZVP ECD spectra of (*R*)-**1** and (*S*)-**1** (average of two solid-state X-ray conformers) computed for the B3LYP/6-31G(d) optimized X-ray conformers indicating mirror-image ECD to the solution results (due to the different conformations)

Figure S4. The chiral-phase HPLC chromatogram of **1**

Figure S5. The chiral-phase HPLC chromatogram of synthetic **1a**

Figure S6. The chiral-phase HPLC chromatogram of synthetic **1b**

Figure S7. ^1H NMR spectrum of compound **1** in CDCl_3

Figure S8. ^{13}C NMR spectrum of compound **1** in CDCl_3

Figure S9. HSQC spectrum of compound **1** in CDCl_3

Figure S10. HMBC spectrum of compound **1** in CDCl_3

Figure S11. COSY spectrum of compound **1** in CDCl_3

Figure S12. NOESY spectrum of compound **1** in CDCl_3

Figure S13. HR-ESI-MS spectrum of compound **1**

Figure S14. IR (KBr disc) spectrum of compound **1**

Figure S15. ECD spectrum of compound **1a**

Figure S16. ECD spectrum of compound **1b**

Figure S17. ^1H NMR spectrum of compound **2** in CDCl_3

Figure S18. ^{13}C NMR spectrum of compound **2** in CDCl_3

Figure S19. ^1H NMR spectrum of precursor of compound **3** in CDCl_3

Figure S20. ^{13}C NMR spectrum of precursor of compound **3** in CDCl_3

Figure S21. ^1H NMR spectrum of compound **4** in CDCl_3

Figure S22. ^{13}C NMR spectrum of compound **4** in CDCl_3

Figure S23. ^1H NMR spectrum of compound **5a** in CDCl_3

Figure S24. ^{13}C NMR spectrum of compound **5a** in CDCl_3

Figure S25. ^1H NMR spectrum of compound **5b** in CDCl_3

Figure S26. ^{13}C NMR spectrum of compound **5b** in CDCl_3

Figure S27. ^1H NMR spectrum of compound **6a** in CDCl_3

Figure S28. ^{13}C NMR spectrum of compound **6a** in CDCl_3

Figure S29. ^1H NMR spectrum of compound **6b** in CDCl_3

Figure S30. ^{13}C NMR spectrum of compound **6b** in CDCl_3

Figure S31. ^1H NMR spectrum of compound **7a** in CDCl_3

Figure S32. ^{13}C NMR spectrum of compound **7a** in CDCl_3

Figure S33. ^1H NMR spectrum of compound **7b** in CDCl_3

Figure S34. ^{13}C NMR spectrum of compound **7b** in CDCl_3

Figure S35. ^1H NMR spectrum of synthetic **1a** in CDCl_3

Figure S36. ^{13}C NMR spectrum of synthetic **1a** in CDCl_3

Figure S37. ^1H NMR spectrum of synthetic **1b** in CDCl_3

Figure S38. ^{13}C NMR spectrum of synthetic **1b** in CDCl_3

Experimental section

1.1. General Experiment Procedures.

Optical rotations were measured on a Perkin–Elmer 341 polarimeter. IR spectra were recorded on a Nicolet 6700 spectrometer in KBr pellets. ECD spectra were measured on BRIGHTTIME Chirascan. NMR spectra were recorded on Varian Mercury-500 NMR spectrometer. The chemical shift (δ) values are given in ppm with TMS as internal standard, and coupling constants (J) are in Hz. ESIMS and HRESIMS data were recorded on Waters 2695–3100 LC-MS and Waters Xevo TOF mass spectrometers. Single crystal X-ray diffraction measurements were conducted on a Bruker Smart Apex II diffractometer with a graphite monochromator. Column chromatography (CC) was performed with silica gel (100–200, 200–300 and 300–400 mesh, Qingdao Marine Chemical Industrials, Qingdao, People’s Republic of China) and MCI gel CHP20P (75–150 μm , Mitsubishi Chemical Industries, Tokyo, Japan). TLC was carried out on precoated silica gel GF254 plates (Yantai Chemical Industrials, Yantai, People’s Republic of China), and the TLC spots were viewed at 254 nm and visualized with 5% H_2SO_4 in EtOH containing 10 mg/mL vanillin followed by heating. Analytical HPLC was performed on a Waters 2695 instrument with an Acquity ELSD detector. Preparative HPLC was performed on a Varian PrepStar system with an Alltech 3000 ELSD. Chromatographic separations were carried out on a Waters Sunfire RP C₁₈, 5 μm , 30 mm \times 150 mm column, using a gradient solvent system composed of H_2O and CH_3CN , with a flow rate of 25.0 mL/min. Chiral-phase separation was performed by K-prep LAB100S (YMC, Japan) on a chiral-phase column Daicel Chiralpak AY-H, 10 μm , 5.0 cm I.D. \times 25.0 cm L column (Daicel Chemical Industries, Ltd., Japan), using a gradient solvent system composing hexane/EtOH/HAc (90:10:0.1). Analytical chiral-phase HPLC was performed by Shimadzu LC 20A QA&QC-HPLC-02 on a chiral-phase column Daicel Chiralpak AY-H, 5 μm , 0.46 cm I.D. \times 15.0 cm L column (Daicel Chemical Industries, Ltd., Japan). All solvents used for CC and HPLC were of analytical grade (Shanghai Chemical Reagents Co. Ltd.) and gradient grade (Merck KGaA), respectively.

1.2. Plant Material

The bark of *C. fortunei* was collected in She County, Anhui Province, China, in October 2013, and identified

by Professor Jin-Gui Shen from the Shanghai Institute of Materia Medica. A voucher specimen (no.20130506) was deposited at the Herbarium of the Shanghai Institute of Materia Medica, Chinese Academy of Sciences.

1.3. Extraction and Isolation

The air-dried and powdered bark of *C. fortunei* (110 kg) was extracted with acetone (3×330L) at room temperature. After evaporation of the solvent, part of the residue (2 kg) was dissolved in water and partitioned with PE, CH₂Cl₂, and EtOAc, successively. The PE fraction was concentrated and then dissolved in 80% aq. MeOH. The CH₂Cl₂ fraction and the MeOH layer were combined together based on the TLC profiles and subjected to CC over MCI gel (EtOH/H₂O, 60% to 95%) to yield 3 fractions (A–C). Fraction A (75 g) was subjected to CC over MCI gel (EtOH/H₂O, 30% to 70%) to give 13 fractions (A1–A13). Fraction A10 (10.8 g) was subjected to CC over silica gel eluting with petroleum ether/acetone (10:1 to 1:2) in a stepwise manner, to afford 16 fractions (A10A–A10P). Subsequently, fraction A10J (753 mg) was selected for separation by preparative HPLC (CH₃CN/H₂O, 35% to 45%) and then further purified by CC over silica gel eluting with CH₂Cl₂/acetone (10:1) to yield Cryptomeriolide (**1**) (44mg).

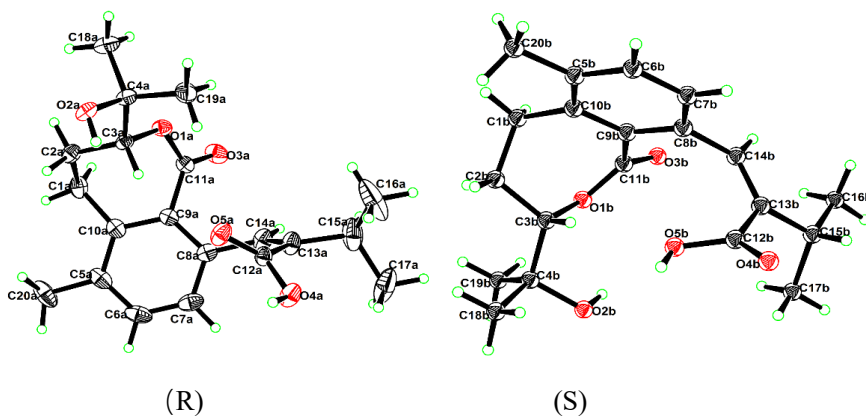
1.4. Characteristics of Compounds

Cryptomeriolide (1): white powder; $[\alpha]_D^{20} + 159$ (*c* 0.3, MeOH) (**1a**), $[\alpha]_D^{20} - 153$ (*c* 0.3, MeOH) (**1b**); ECD (MeOH) λ_{\max} ($\Delta\epsilon$) 248 (+ 30.35), 233 (0), 222 (– 25.75), 212 (0), 196 (+ 42.76) nm (**1a**), ECD (MeOH) λ_{\max} ($\Delta\epsilon$) 248 (– 33.42), 233 (0), 222 (+ 28.43), 212 (0), 197 (– 47.03) nm (**1b**); IR (KBr) ν_{\max} 3446, 2965, 2928, 2871, 1713, 1466, 1384, 1261, 1182, 1090, 1053, 802 cm^{–1}; ¹H and ¹³C NMR: see Table 1; ESI–MS *m/z* 347.3 [M+H]⁺, 345.2 [M – H][–], 691.4 [2M – 1][–]; ESI–HRMS *m/z* 369.1662 [M+Na]⁺ (calcd for C₂₀H₂₆O₅Na, 369.1672).

1.5. X-ray Crystallographic Analysis of Compound 1

Cryptomeriolide (1) was cultivated upon slow evaporation of the mixture (CH₂Cl₂-*n*-hexane) by keeping the sample at room temperature. The structure was solved and refined using the Bruker SHELXTL Software Package. Crystallographic data for **1** (key parameters see Tables S1) have been deposited at the Cambridge Crystallographic Data Centre (Deposition Nos.: CCDC 1446792). Copies of these data can be obtained free of charge via the internet at www.ccdc.cam.ac.uk/conts/retrieving.html or on application to CCDC, 12 Union Road, Cambridge CB2 1EZ, UK [Tel: (+44) 1223-336-408; Fax: (+44) 1223-336-033; E-mail: deposit@ccdc.cam.ac.uk].

X-ray crystal data for compound **1**



Empirical Formula	C ₄₀ H ₅₂ O ₁₀
Formula weight	692.82
Temperature	170K
Wavelength	0.71073
Crystal system	Triclinic
Space group	P -1
Unit cell dimensions	$a = 12.8671(3) \text{ \AA}$ $\alpha = 64.1960(10)^\circ$. $b = 14.1050(3) \text{ \AA}$ $\beta = 89.7430(10)^\circ$. $c = 15.2457(3) \text{ \AA}$ $\gamma = 63.3900(10)^\circ$.
Volume	2163.93(8) \AA^3
Z	2
Density (calculated)	1.063 Mg/m ³
Absorption coefficient	0.076 mm ⁻¹
F (000)	744
Theta range for data collection	1.53 to 27.45°
Index ranges	-16 ≤ h ≤ 16, -18 ≤ k ≤ 15, -19 ≤ l ≤ 19
Reflections collected	35529
Independent reflections	9837 [R(int) = 0.0406]
Data/restraints/parameters	9837/0/461
Goodness-of-fit on F ²	1.022
Final R indices [I > 2σ(I)]	R1 = 0.0592, wR2 = 0.1687
R indices (all data)	R1 = 0.0986, wR2 = 0.1842

Largest diff. peak/hole 0.477/-0.375 e.Å⁻³

Completeness 0.994

1.6. Chiral-phase Separation of **1**

Compound **1** was separated by K-prep LAB100S (YMC, Japan) on a chiral-phase column Daicel Chiralpak AY-H, 10 μ m, 5.0 cm I.D. \times 250 cm L column (Daicel Chemical Industries, Ltd., Japan). The mobile phase consisted of Hexane/EtOH/HAc (90:10:0.1) with a flow rate of 1.0ml/min. The detection wavelength was at 240 nm. Their peak areas are almost identical with a ratio of 1:1.

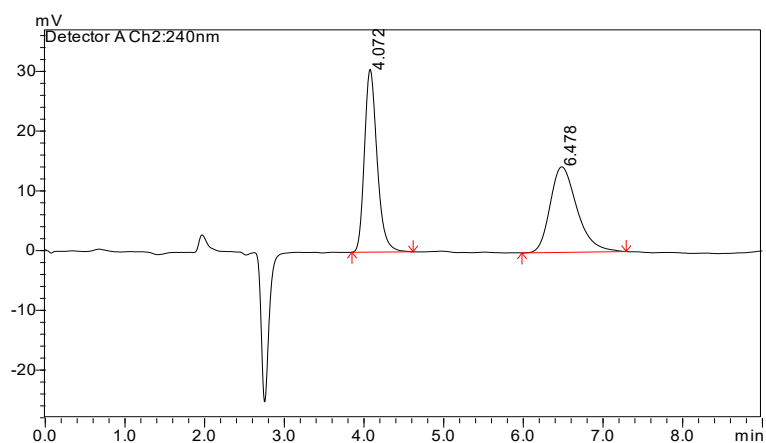


Figure S1 The chiral-phase HPLC chromatogram of **1**

Peak#	Ret. Time	Area	Area%	T.Plate#	Tailing F.	Resolution
1	4.072	338938	50.2238	3098.224	1.307	--
2	6.478	335917	49.7762	1824.661	1.349	5.350

1.7. Computational Methods for ECD of Compounds **1a**, **1b**

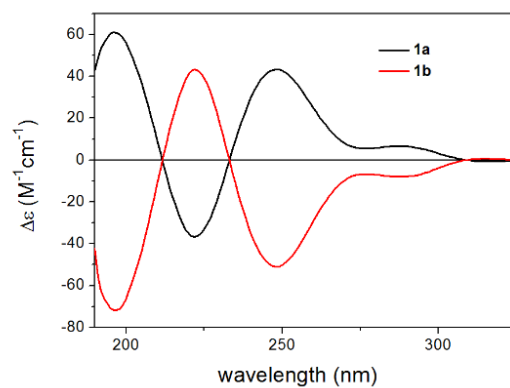


Figure S2. Experimental ECD spectra of (+)-**1a** and (-)-**1b** in MeOH.

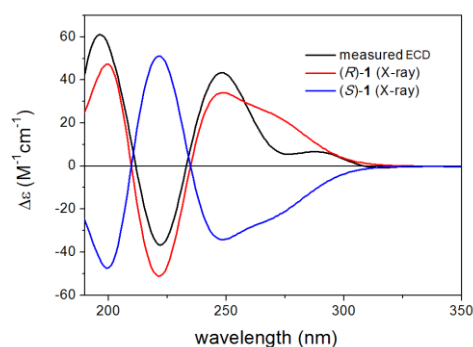


Figure S3. Experimental ECD spectrum of 1a in MeOH (black) compared with the BH&HLYP/TZVP ECD spectra of (R)-1 and (S)-1 (average of two solid-state X-ray conformers) computed for the B3LYP/6-31G(d) optimized X-ray conformers indicating mirror-image ECD to the solution results (due to the different conformations).

Table 1. Boltzmann populations and optical rotations of the low-energy conformers of (S)-1 computed at various levels with PCM for MeOH for the CAM-B3LYP/TZVP PCM/MeOH reoptimized MMFF conformers.

Conformer	Boltzmann population	B3LYP/TZVP	BH&HLYP/TZVP	CAM-B3LYP/TZVP	PBE0/TZVP
Conf. A	28.01 %	269.28	232.14	238.51	269.51
Conf. B	17.40 %	263.57	226.60	231.85	263.83
Conf. C	11.01 %	262.07	223.83	228.60	263.29
Conf. D	6.79 %	255.10	217.29	220.94	256.47
Conf. E	5.08 %	249.22	215.30	209.88	248.09
Conf. F	3.40 %	264.61	225.22	230.86	263.61
Conf. G	2.36 %	264.49	226.19	231.66	265.17
Conf. H	2.10 %	215.95	192.10	182.39	218.48
Conf. I	2.01 %	268.22	232.52	237.49	268.30
Conf. J	1.86 %	275.21	237.58	242.58	275.68
Conf. K	1.68 %	279.55	238.34	231.16	277.72
Conf. L	1.65 %	244.10	210.74	213.95	245.37
Conf. M	1.61 %	263.85	227.50	231.42	264.45
Conf. N	1.55 %	254.31	219.75	224.27	254.45
Conf. O	1.43 %	251.79	217.29	221.49	252.66
Conf. P	1.00 %	252.19	214.16	217.89	249.17
Conf. Q	0.96 %	307.75	260.78	253.49	304.53
Average	N/A	262.95	226.04	230.04	263.26

Computational Section. Mixed torsional/low-frequency mode conformational searches were carried out by means of the Macromodel 10.8.011 software using the Merck Molecular Force Field (MMFF).¹ Geometry reoptimizations at the B3LYP/6-31G(d) level in vacuo, the B97D/TZVP PCM/MeOH and the CAM-B3LYP/TZVP PCM/MeOH, the TDDFT ECD calculations and the OR calculations run with various functionals (B3LYP, BH&HLYP, CAM-B3LYP, PBE0) and the TZVP basis set were performed with the Gaussian 09 package.² ECD spectra were generated as sums of Gaussians with 3000 cm⁻¹ half-height widths (corresponding to ca. 15 nm at 220

nm), using dipole-velocity-computed rotational strength values.³ Boltzmann distributions were estimated from the ZPVE corrected B3LYP energies and the uncorrected B97D and CAM-B3LYP energies. X-ray geometries were taken as 1:1 ratio. The MOLEKEL software package was used for visualization of the results.⁴

¹ MacroModel; Schrödinger, LLC, 2015, <http://www.schrodinger.com/MacroModel>.

² Frisch, M. J.; Trucks, G. W.; Schlegel, H. B.; Scuseria, G. E.; Robb, M. A.; Cheeseman, J. R.; Scalmani, G.; Barone, V.; Mennucci, B.; Petersson, G. A.; Nakatsuji, H.; Caricato, M.; Li, X.; Hratchian, H. P.; Izmaylov, A. F.; Bloino, J.; Zheng, G.; Sonnenberg, J. L.; Hada, M.; Ehara, M.; Toyota, K.; Fukuda, R.; Hasegawa, J.; Ishida, M.; Nakajima, T.; Honda, Y.; Kitao, O.; Nakai, H.; Vreven, T.; Montgomery, J. A., Jr.; Peralta, J. E.; Ogliaro, F.; Bearpark, M.; Heyd, J. J.; Brothers, E.; Kudin, K. N.; Staroverov, V. N.; Kobayashi, R.; Normand, J.; Raghavachari, K.; Rendell, A.; Burant, J. C.; Iyengar, S. S.; Tomasi, J.; Cossi, M.; Rega, N.; Millam, J. M.; Klene, M.; Knox, J. E.; Cross, J. B.; Bakken, V.; Adamo, C.; Jaramillo, J.; Gomperts, R.; Stratmann, R. E.; Yazyev, O.; Austin, A. J.; Cammi, R.; Pomelli, C.; Ochterski, J. W.; Martin, R. L.; Morokuma, K.; Zakrzewski, V. G.; Voth, G. A.; Salvador, P.; Dannenberg, J. J.; Dapprich, S.; Daniels, A. D.; Farkas, O.; Foresman, J. B.; Ortiz, J. V.; Cioslowski, J.; Fox, D. J. Gaussian 09, revision B.01; Gaussian, Inc.: Wallingford, CT, 2010.

³ Stephens, P. J.; Harada, N. Chirality 2010, 22, 229-233.

⁴ Varetto, U. MOLEKEL, v. 5.4; Swiss National Supercomputing Centre: Manno, Switzerland, 2009.

1.8. Enantioselective Synthesis of 1a and 1b

1.8.1. Methylation and oxidation of sugiol

1.07 g of sugiol (3.57 mmol) and 984 g of anhydrous K₂CO₃ (7.13 mmol, 2.0 eq.) was suspended in 20 ml of dry acetone/THF. To this mixture solution 674 μ l of Me₂SO₄ (7.13 mmol, 2.0 eq.) was added. The reaction mixture was stirred at room temperature for overnight, diluted with water and then extracted with ethyl acetate (100 ml \times 3). The organic layer was combined and dried with MgSO₄. After evaporation under reduced pressure, the residue was purified on silica gel column chromatography (PE:EE 100:2-100:6) to afford methylation product 987 mg (ESIMS *m/z* 315.3 [M+H]⁺).

A mixture of methylation product (987 mg, 3.14 mmol) and SeO₂ (3.95 g, 35.6 mmol, 11.2 eq.) in acetic acid (30 ml) and water (10 ml) was refluxed for 2.5 h. The cooled mixture was diluted with dichloromethane (150 ml) and washed with saturated NaHCO₃ solution (300 ml \times 3), brine (100 ml). The organic solvent was evaporated and the residue was purified by column chromatography (PE:EE 100:4-100:10) to yield oxidation product **2** (905 mg, yield 85%).

¹H-NMR (400 MHz, CDCl₃) δ 7.99 (1H, s), 6.85 (1H, s), 6.45 (1H, s), 3.89 (3H, s), 3.28 (1H, m), 2.14 (1H, m), 2.03 (1H, m), 1.64-1.77 (3H, m), 1.54 (3H, s), 1.43 (1H, m), 1.26 (3H, s), 1.25 (3H, d, *J* = 6.9 Hz), 1.22 (3H, d, *J* = 6.9 Hz); ¹³C-NMR (100 MHz, CDCl₃) δ 185.1 (s), 172.6 (s), 160.7 (s), 153.7 (s), 135.9 (s), 124.5 (d), 124.0 (d), 123.4 (s), 105.5 (d), 55.3 (q), 41.3 (s), 40.2 (t), 37.8 (t), 37.4 (s), 32.6 (q), 32.4 (q), 29.1 (q), 26.6 (d), 22.5 (q), 22.3 (q), 18.6 (t); ESI-MS: *m/z* 313.3 [M+H]⁺.

1.8.2. Demethylation, acetylation and reduction of **2**

2 (900 mg, 2.88 mmol) and ethanethiol (2.16 ml, 1.86 g, 30 mmol, 7.5 eq.) were dissolved in 15 ml of dry dichloromethane in a 50 ml of flask. The solution was cooled in an ice-water bath and then anhydrous aluminum chloride (16.1 mmol, 2.15 g, 4.0 eq.) was added over a 10-min period. After stirring at this temperature for 10 min and at room temperature for 2 h, the mixture was poured into diluted HCl at 0 °C and extracted with ether (50 ml \times 3). The combined organic layer was washed with brine, dried over MgSO₄ and evaporated under reduced pressure. The residue was used for next step without further purification.

The above residue and acetic anhydride in 10 ml of dry pyridine was allowed at room temperature for overnight. The mixture was neutralized and extracted with ethyl acetate (50 ml \times 3). The organic layer was washed with brine, dried over MgSO₄ and evaporated in vacuum. The residue was subjected to a silica gel column eluting with PE:EE 100:4 to afford acetyl product (868.8 mg, 96%),

¹H-NMR (400 MHz, CDCl₃) δ 8.10 (1H, s), 7.14 (1H, s), 6.48 (1H, s), 3.03 (1H, m), 2.38 (1H, br.d), 2.35 (3H, s), 2.14 (1H, m), 2.01 (1H, m), 1.63-1.75 (3H, m), 1.53 (3H, s), 1.43 (1H, m), 1.35 (3H, s), 1.26 (3H, d, J = 6.8 Hz), 1.26 (3H, s), 1.23 (3H, d, J = 6.8 Hz); ¹³C-NMR (100 MHz, CDCl₃) δ 185.0 (s), 173.8 (s), 169.1 (s), 152.6 (s), 151.8 (s), 138.8 (s), 128.3 (s), 124.9 (d), 124.4 (d), 118.9 (d), 41.1 (s), 40.1 (t), 37.5 (s), 37.4 (t), 32.6 (q), 32.5 (q), 29.1 (q), 27.4 (d), 22.8 (q), 22.7 (q), 21.0 (q), 18.4 (t); ESIMS m/z 341.3 [M+H]⁺.

1.8.3. A-ring open reaction of **3**

The above acetyl product (868.8 g, 2.55 mmol) and cerium (III) chloride heptahydrate (1.07 mg, 2.88 mmol) were dissolved in anhydrous THF (7 ml) and methanol (3 ml) in a 100 ml of flask. To this solution NaBH₄ (109 mg, 2.88 mmol) was added at room temperature. The reaction mixture was further stirred at room temperature for 30 min and quenched by NHCl₄. The mixture was diluted with ether and the precipitation was filtered. The filtrate was washed with brine, dried over MgSO₄, and evaporated under reduced pressure to give a crude alcohol **3** (0.90 g), which was used for next step without further purification.

The above crude alcohol was treated with p-toluenesulfonic acid (150 mg, 0.78 mmol) in 30 ml of benzene at 85 °C for 2 hours. The solution was cooled to room temperature and diluted with ether. The organic layer was washed with saturated NaHCO₃ (20 ml) for twice, dried with MgSO₄ and concentrated under reduced pressure. The residue was purified on a silica gel column eluting with PE:EE 100:2 to give the A-ring open product **4** (422 mg, yield 48%).

¹H-NMR (400 MHz, CDCl₃) δ 7.69 (1H, s), 7.63 (1H, s), 7.58 (1H, d, J = 8.3 Hz), 7.25 (1H, d, J = 8.3 Hz), 5.31 (1H, m), 3.11 (1H, m), 3.01 (2H, m), 2.48 (3H, s), 2.40 (3H, s), 2.30 (2H, m), 1.73 (3H, s), 1.59 (3H, s), 1.32 (6H, d, J = 7.9 Hz); ¹³C-NMR (100 MHz, CDCl₃) δ 169.3 (s), 146.7 (s), 137.5 (s), 134.4 (s), 132.2 (s), 131.7 (s), 130.7

(s), 130.6 (s), 128.5 (d), 125.6 (d), 125.0 (d), 123.5 (d), 115.4 (d), 28.5 (t), 28.0 (t), 27.3 (q), 25.2 (d), 25.2 (q), 22.6 (q), 20.6 (q), 19.6 (q), 17.1 (q); ESI-MS: m/z 313.3 $[M+H]^+$.

1.8.4. Oxidation of **4**

According to the method of Sharpless, 109 mg of **4** (0.34 mmol) and methane-sulfonamide (32 mg, 0.33 mmol) were dissolved in 4 ml of water and 4 ml of *t*BuOH, AD-mix- α (476 mg, 1.4 g/mmol) was added at room temperature. The reaction mixture was stirred vigorously at room temperature for overnight, was quenched with saturated aqueous Na_2SO_3 solution (60 mL). Then the mixture was extracted with EtOAc (100 ml \times 3), washed with brine (100 ml), dried over MgSO_4 , and then concentrated under reduced pressure. The residue was purified on silica gel column eluting with PE:EE (5:2) to afford the title product **5a** (52 mg, 47%) as light yellow solid. ^1H -NMR (400 MHz, CDCl_3) δ 7.77 (1H, s), 7.68 (1H, s), 7.58 (1H, d, J = 8.4 Hz), 7.25 (1H, d, J = 8.4 Hz), 3.40 (1H, br.d, J = 8.0 Hz), 3.26 (1H, m), 3.12 (2H, m), 2.49 (3H, s), 2.39 (3H, s), 1.67 (1H, m), 1.60 (1H, m), 1.32 (3H, d, J = 6.9 Hz), 1.31 (3H, d, J = 6.9 Hz), 1.14 (3H, s), 1.11 (3H, s); ^{13}C -NMR (100 MHz, CDCl_3) δ 170.0 (s), 147.0 (s), 137.9 (s), 134.9 (s), 132.9 (s), 131.3 (s), 131.0 (s), 129.1 (d), 126.0 (d), 125.6 (d), 116.0 (d), 78.0 (d), 73.1 (s), 31.7 (t), 27.8 (d), 26.4 (q), 25.4 (t), 23.3 (q), 23.0 (q), 23.0 (q), 21.3 (q), 20.0 (q); ESIMS m/z 381.2 $[M+\text{Na}]^+$.

Following the same procedure, 269 mg of **4** (0.86 mmol) was treated with AD-mix- β (1.162 g, 1.4 g/mmol) to yield 160 mg of **5b** (59%). ^1H -NMR (400 MHz, CDCl_3) δ 7.78 (1H, s), 7.68 (1H, s), 7.58 (1H, d, J = 8.3 Hz), 7.25 (1H, d, J = 8.3 Hz), 3.40 (1H, dd, J = 1.9, 8.0 Hz), 3.27 (1H, m), 3.13 (2H, m), 2.49 (3H, s), 2.39 (3H, s), 1.76 (1H, m), 1.66 (1H, m), 1.32 (3H, d, J = 6.9 Hz), 1.31 (3H, d, J = 6.9 Hz), 1.13 (3H, s), 1.11 (3H, s); ^{13}C -NMR (100 MHz, CDCl_3) δ 170.0 (s), 147.0 (s), 137.9 (s), 134.9 (s), 132.9 (s), 131.2 (s), 131.0 (s), 129.1 (d), 126.0 (d), 125.6 (d), 116.0 (d), 78.0 (d), 73.1 (s), 31.7 (t), 27.8 (d), 26.4 (q), 25.4 (t), 23.3 (q), 23.0 (q), 23.0 (q), 21.3 (q), 20.0 (q); ESIMS m/z 381.2 $[M+\text{Na}]^+$.

1.8.5. Diol protection and deacetylation of **5**

To a solution of the chiral diol **5** (140 mg, 0.391 mmol) in 3.0 mL of dichloromethane were added (\pm)-10-camphorsulfonic acid (4.5 mg, 20 μmol , 0.05 eq.) and 2,2-dimethoxypropane (0.144 mL, 1.173 mmol, 3 eq.) at 0 $^\circ\text{C}$ under a nitrogen atmosphere, and the mixture was stirred at room temperature for 1 h. A saturated aqueous solution of NaHCO_3 (5 mL) was added, and the aqueous layer was extracted with dichloromethane (5 mL \times 3). The organic layer was combined and evaporated, the residue was purified by CC (PE:EE 100:6) to yield diol protected product **6** 126 mg (90%), ESIMS m/z 399.2 $[M+H]^+$.

The diol protected product **6** was dissolved in 5 mL of dry THF and LiAlH_4 powder was added at 0 $^\circ\text{C}$. The reaction mixture was stirred for 1 hour, poured into a cooled HCl solution (1 M), and extracted with ether. The

combined organic phase was washed with brine and dried with MgSO₄, evaporated in vacuum. The residue was purified by CC (PE:EE 5:1) to give an oily product **7** (100 mg, 80%).

6a: ¹H-NMR (400 MHz, CDCl₃) δ 7.69 (1H, s), 7.69 (1H, s), 7.59 (1H, d, J = 8.4 Hz), 7.25 (1H, d, J = 8.4 Hz), 3.79 (1H, dd, J = 2.5, 10.3 Hz), 3.27 (1H, m), 3.08 (2H, m), 2.50 (3H, s), 2.39 (3H, s), 1.80 (1H, m), 1.65 (1H, m), 1.49 (3H, s), 1.39 (3H, s), 1.32 (3H, d, J = 6.8 Hz), 1.31 (3H, d, J = 6.8 Hz), 1.21 (3H, s), 1.07 (3H, s); ¹³C-NMR (100 MHz, CDCl₃) δ 169.9 (s), 147.4 (s), 138.2 (s), 134.6 (s), 133.0 (s), 131.3 (s), 131.2 (s), 129.1 (d), 126.2 (d), 125.9 (d), 116.1(d), 106.9 (s), 83.1 (d), 80.3 (s), 29.8 (t), 28.8 (q), 27.9 (d), 27.1 (q), 26.1 (t), 25.9 (q), 23.2 (q), 23.1 (q), 23.1 (q), 21.2 (q), 20.2 (q); ESIMS m/z 399.3 [M+H]⁺.

6b: ¹H-NMR (400 MHz, CDCl₃) δ 7.69 (1H, s), 7.68 (1H, s), 7.59 (1H, d, J = 8.4 Hz), 7.26 (1H, d, J = 8.4 Hz), 3.79 (1H, dd, J = 2.5, 10.3 Hz), 3.27 (1H, m), 3.08 (2H, m), 2.50 (3H, s), 2.39 (3H, s), 1.80 (1H, m), 1.66 (1H, m), 1.49 (3H, s), 1.39 (3H, s), 1.32 (3H, d, J = 6.9 Hz), 1.31 (3H, d, J = 6.9 Hz), 1.21 (3H, s), 1.06 (3H, s); ¹³C-NMR (100 MHz, CDCl₃) δ 169.9 (s), 147.4 (s), 138.2 (s), 134.6 (s), 133.0 (s), 131.3 (s), 131.2 (s), 129.1 (d), 126.2 (d), 125.9 (d), 116.1(d), 106.9 (s), 83.1 (d), 80.3 (s), 29.8 (t), 28.8 (q), 27.9 (d), 27.1 (q), 26.1 (t), 25.9 (q), 23.2 (q), 23.1 (q), 23.1 (q), 21.2 (q), 20.2 (q); ESIMS m/z 399.2 [M+H]⁺.

7a: ¹H-NMR (400 MHz, CDCl₃) δ 7.59 (1H, s), 7.54 (1H, d, J = 8.3 Hz), 7.31 (1H, s), 7.14 (1H, d, J = 8.3 Hz), 5.39 (1H, br.s), 3.83 (1H, dd, J = 2.5, 10.2 Hz), 3.34 (1H, m), 3.24 (1H, m), 3.04 (1H, m), 2.49 (3H, s), 1.84 (1H, m), 1.63 (1H, s), 1.52 (3H, s), 1.36 (3H, d, J = 6.9 Hz), 1.35 (3H, d, J = 6.9 Hz), 1.23 (3H, s), 1.08 (3H, s); ¹³C-NMR (100 MHz, CDCl₃) δ 152.5 (s), 135.5 (s), 132.9 (s), 132.8 (s), 131.8 (s), 128.4 (s), 126.9 (d), 126.0 (d), 125.9 (d), 107.0 (s), 106.0 (d), 83.4 (d), 80.5 (s), 29.5 (t), 28.9 (q), 27.6 (d), 27.1 (q), 26.3 (t), 26.1 (q), 23.2 (q), 22.8 (q), 22.7 (q), 20.3 (q); ESIMS m/z 357.2 [M+H]⁺.

7b: ¹H-NMR (400 MHz, CDCl₃) δ 7.59 (1H, s), 7.54 (1H, d, J = 8.3 Hz), 7.31 (1H, s), 7.14 (1H, d, J = 8.3 Hz), 5.44 (1H, s), 3.83 (1H, dd, J = 2.6, 10.2 Hz), 3.34 (1H, m), 3.24 (1H, m), 3.04 (1H, m), 2.48 (3H, s), 1.85 (1H, m), 1.64 (1H, m), 1.52 (3H, s), 1.42 (3H, s), 1.36 (3H, d, J = 6.9 Hz), 1.35 (3H, d, J = 6.9 Hz), 1.22 (3H, s), 1.08 (3H, s); ¹³C-NMR (100 MHz, CDCl₃) δ 152.5 (s), 135.5 (s), 132.9 (s), 132.8 (s), 131.8 (s), 128.4 (s), 126.9 (s), 126.0 (d), 125.9 (d), 107.0 (s), 106.0 (d), 83.4 (d), 80.4 (s), 29.5 (t), 28.9 (q), 27.6 (d), 27.1 (q), 26.3 (t), 26.1 (q), 23.2 (q), 22.8 (q), 22.7 (q), 20.3 (q); ESIMS m/z 357.2 [M+H]⁺.

1.8.6. Oxidation of **7**

82 mg of **7** (0.23 mmol) was dissolved in 8 ml of DMF in a 50 ml flask. The solution was stirred at room temperature in dark (protected with aluminum foil). To this solution was added the Fremy's salt (potassium nitrosodisulfonate) (308 mg) and potassium dihydrogenphosphate (118 mg) in 6 ml water. The mixture was stirred

at rt under a stream nitrogen for 1.5 h and then was treated as above with a solution of Fremy's salt (156 mg) and potassium dihydrogenphosphate (60 mg) in DMF (4 ml) and water (6 ml) for nother 1.5 h. The mixture was poured into diluted HCl and extracted with ether. The ether extract was washed with brine, dried, and evaporated in vacuum. The crude product **8** was used for next step without further purification.

1.8.7. C-ring open of **8**

A solution of *m*-CPBA (85%, 40 mg, 0.187 mmol) in CH₂Cl₂ (5 mL) was added into a solution of **7** (63 mg, 0.17 mmol) in CH₂Cl₂ (10 mL) at 0°C. The resulting mixture was stirred for 2 days at room temperature and concentrated. A solution of the residue in THF (5 mL), was mixed with 10% aqueous HCl (2 mL) at room temperature. The resulting mixture was stirred at room temperature for 48hours, concentrated and purified by preparative HPLC, providing **1** as a white solid (**1a**, 50%; **1b**, 30%).

Synthetic **1a**: white powder; $[\alpha]^{20}_D +148$ (c 0.6, MeOH)

Synthetic **1b**: white powder; $[\alpha]^{20}_D -132$ (c 0.6, MeOH)

1.9. Chiral-phase Analysis of Synthetic **1a** and **1b**

Compounds **1**, **1a** and **1b** were analyzed by Shimadzu LC 20A QA&QC-HPLC-02 on a chiral-phase column Daicel Chiralpak AY-H, 5 μ m, 0.46 cm I.D. \times 15 cm L column (Daicel Chemical Industries, Ltd., Japan). The mobile phase consisted of n-Hexane/ Ethanol /Trifluoroacetic acid (90:10:0.1) with a flow rate of 1.0ml/min. The detection wavelength was at 240 nm.

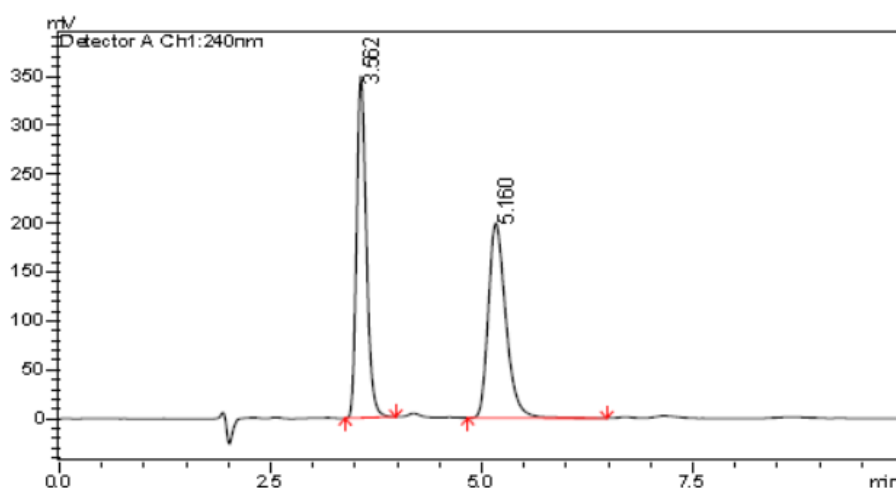


Figure S4 The chiral-phase HPLC chromatogram of **1**

Peak#	Ret.Time	Area	Area%	T.Plate#	Tailing F.	Resolution
1	3.562	2809150	49.2801	3524.368	1.349	—
2	5.160	2891223	50.7199	2734.317	1.381	5.034

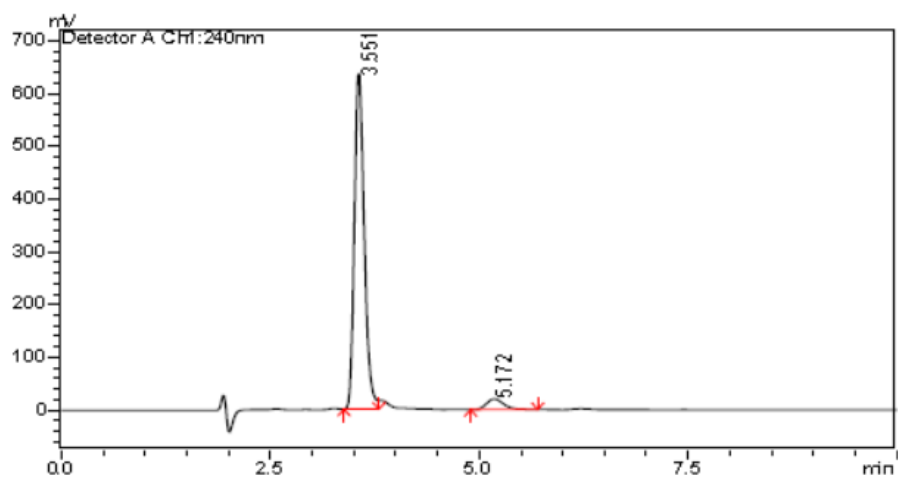


Figure S5 The chiral-phase HPLC chromatogram of synthetic **1a**

Peak#	Ret.Time	Area	Area%	T.Plate#	Tailing F.	Resolution
1	3.551	5243521	94.8252	3493.482	1.372	—
2	5.172	286148	5.1748	2770.018	1.316	5.117

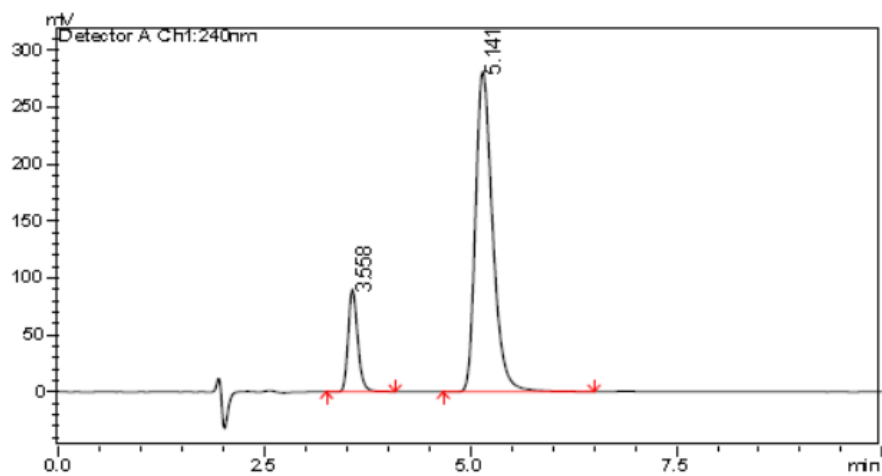


Figure S6 The chiral-phase HPLC chromatogram of synthetic **1b**

Peak#	Ret.Time	Area	Area%	T.Plate#	Tailing F.	Resolution
1	3.558	726462	15.1347	3603.409	1.324	—
2	5.141	4073517	84.8653	2711.484	1.394	5.010

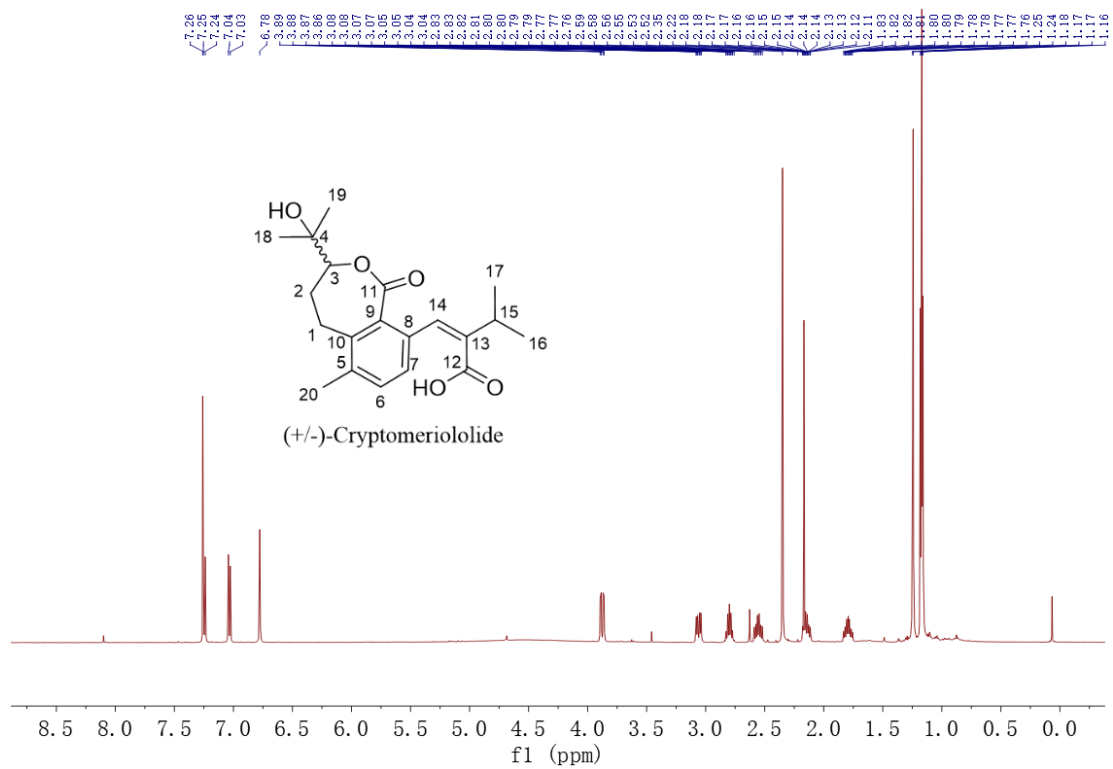


Figure S7. ¹H NMR spectrum of compound **1** in CDCl₃

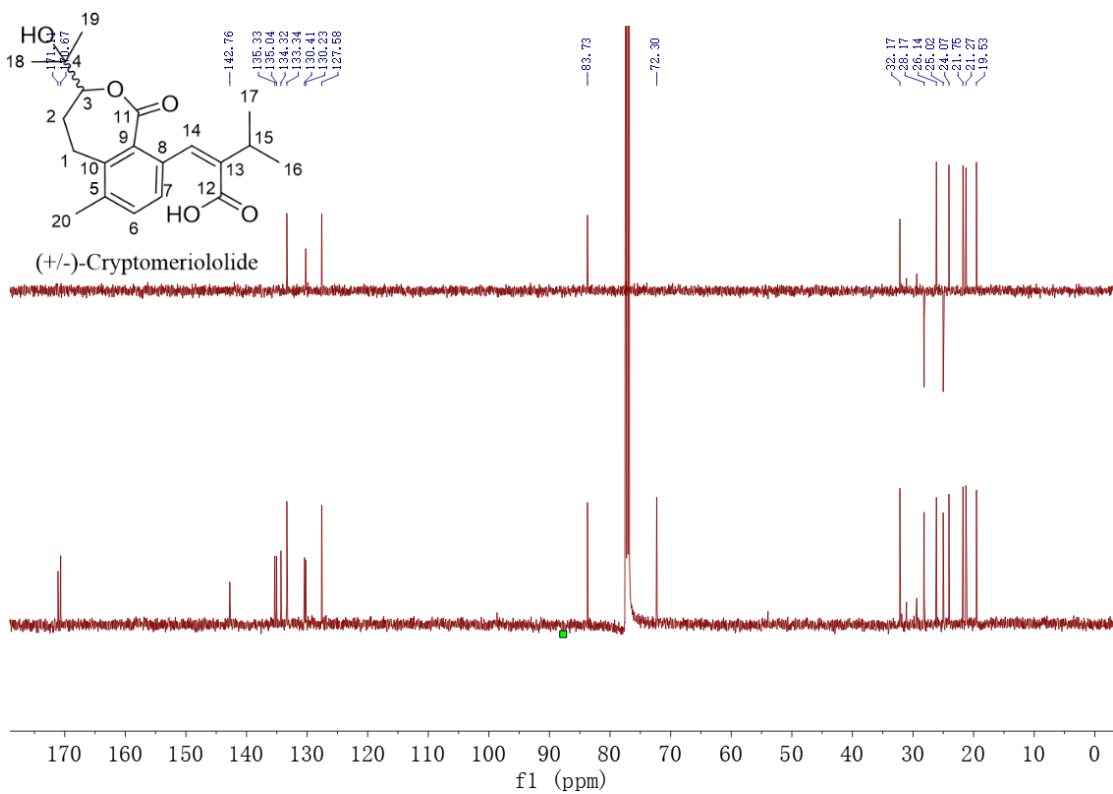


Figure S8. ¹³C NMR spectrum of compound **1** in CDCl₃

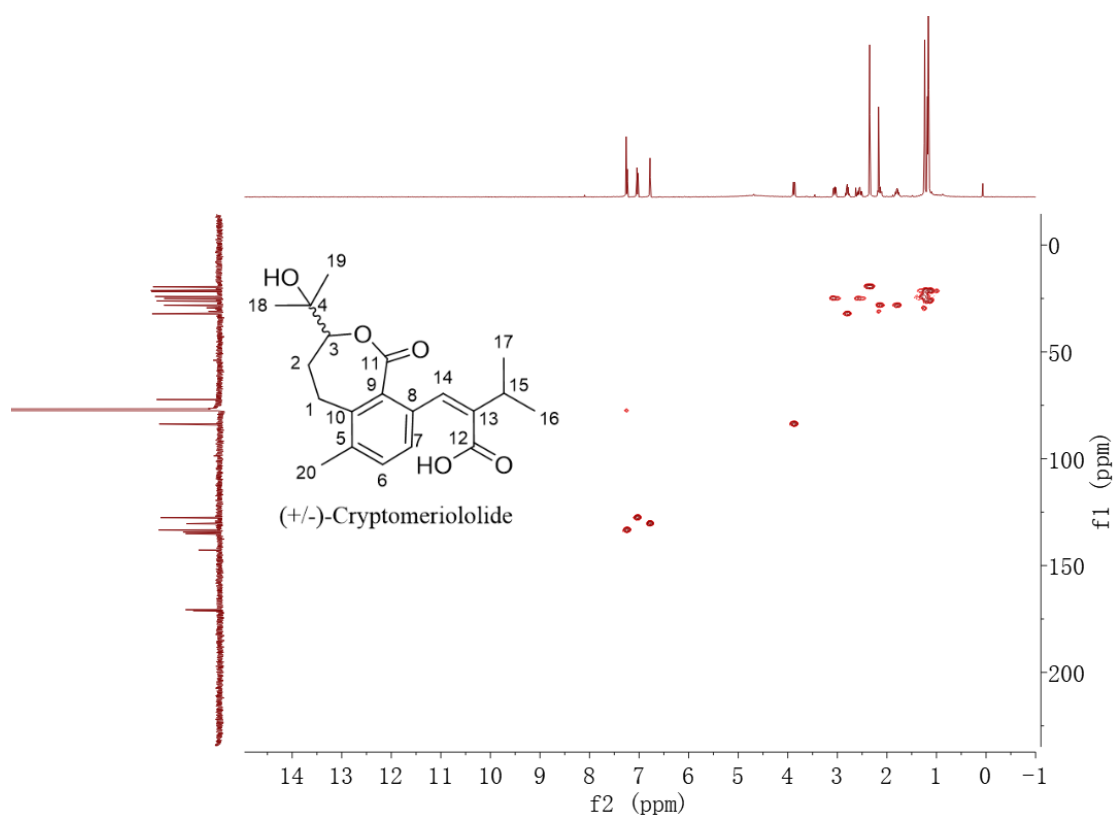


Figure S9. HSQC spectrum of compound **1** in CDCl_3

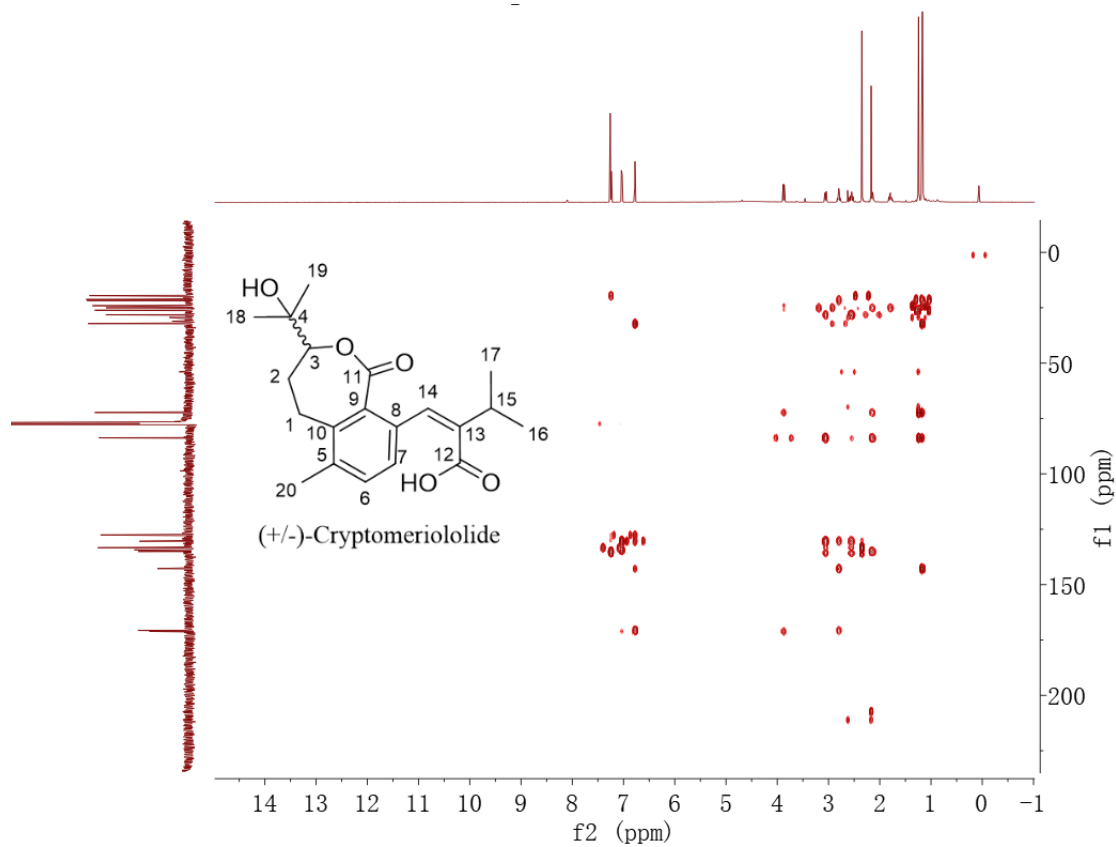


Figure S10. HMBC spectrum of compound **1** in CDCl_3

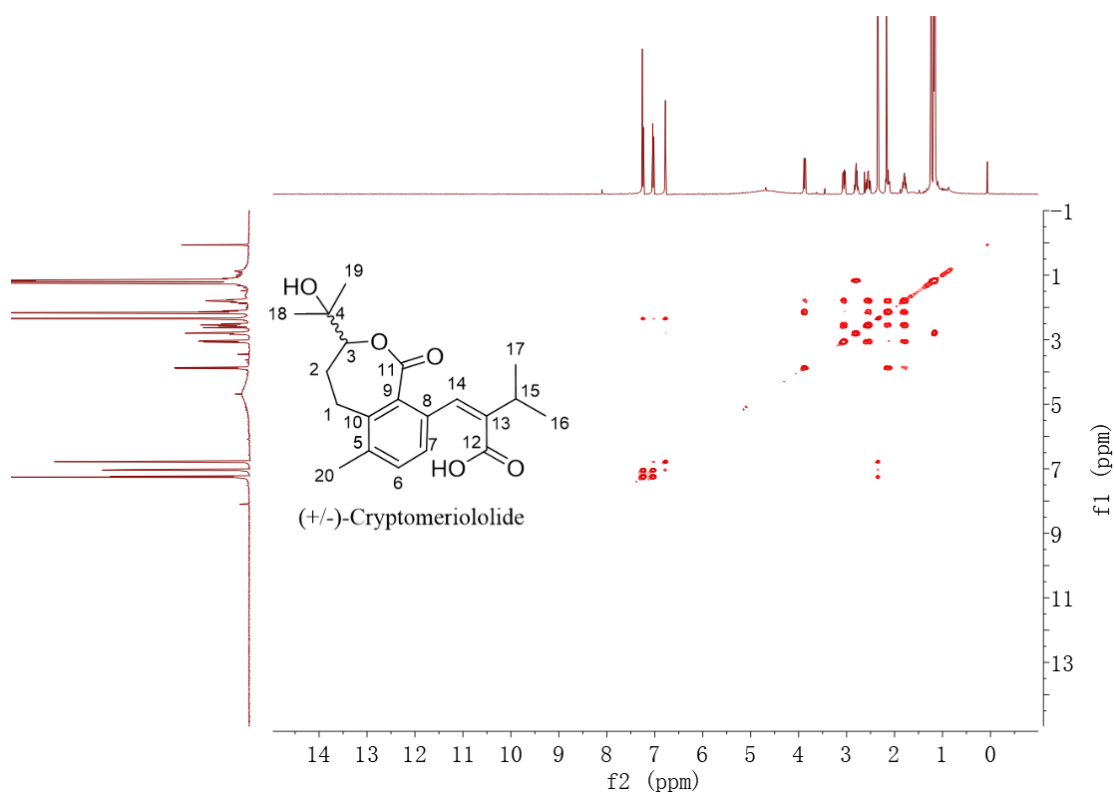


Figure S11. ^1H - ^1H COSY spectrum of compound **1** in CDCl_3

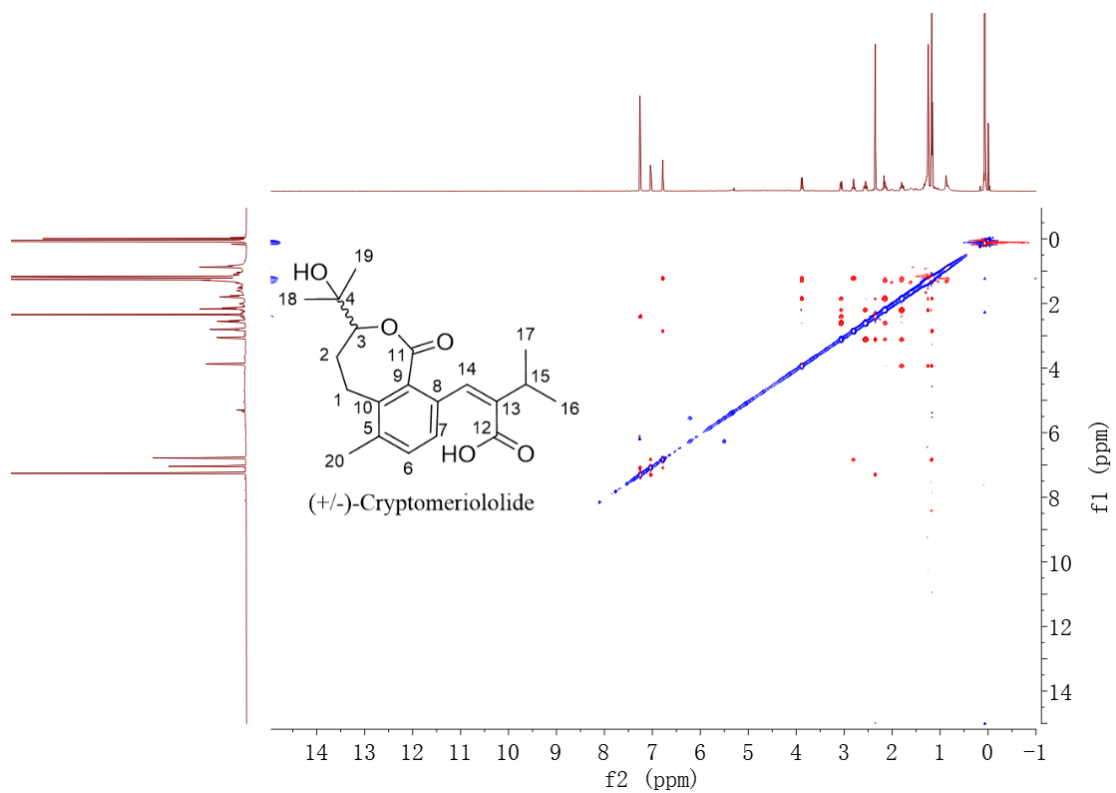


Figure S12. NOESY spectrum of compound **1** in CDCl_3

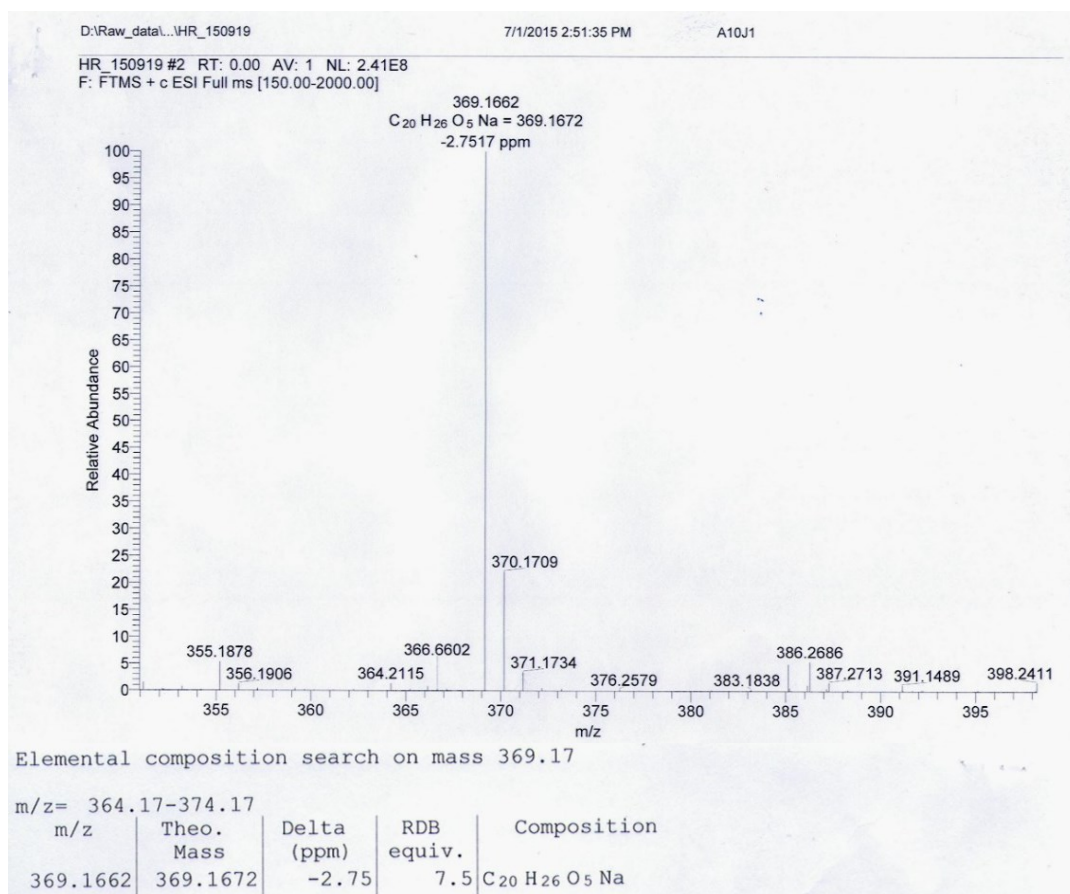


Figure S13. HR-ESI-MS spectrum of compound **1**

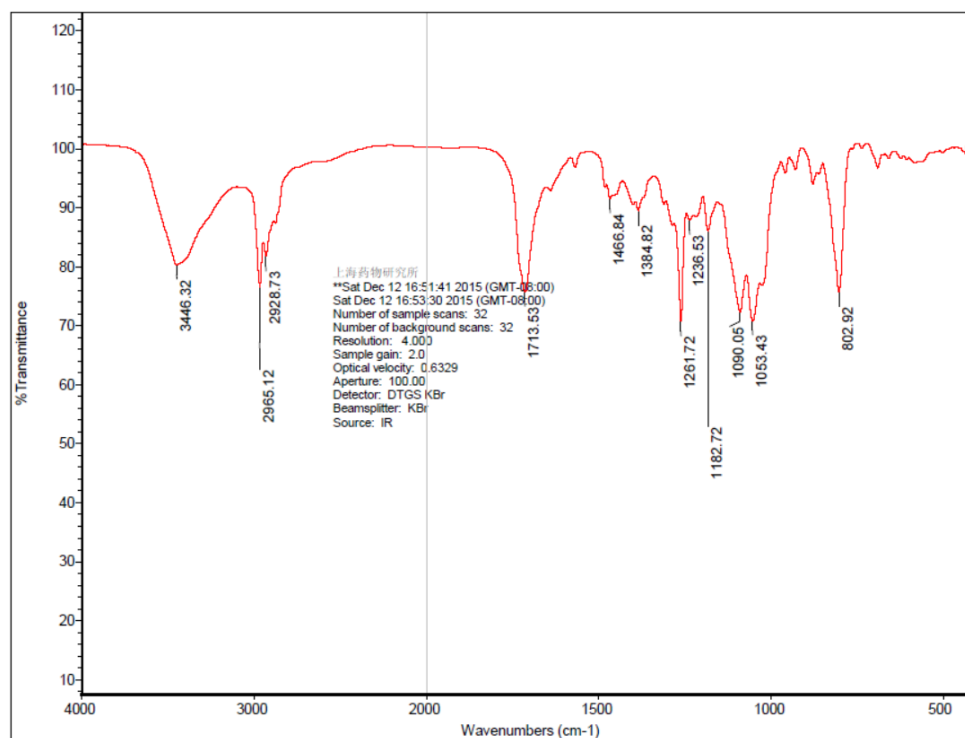


Figure S14. IR (KBr disc) spectrum of compound **1**

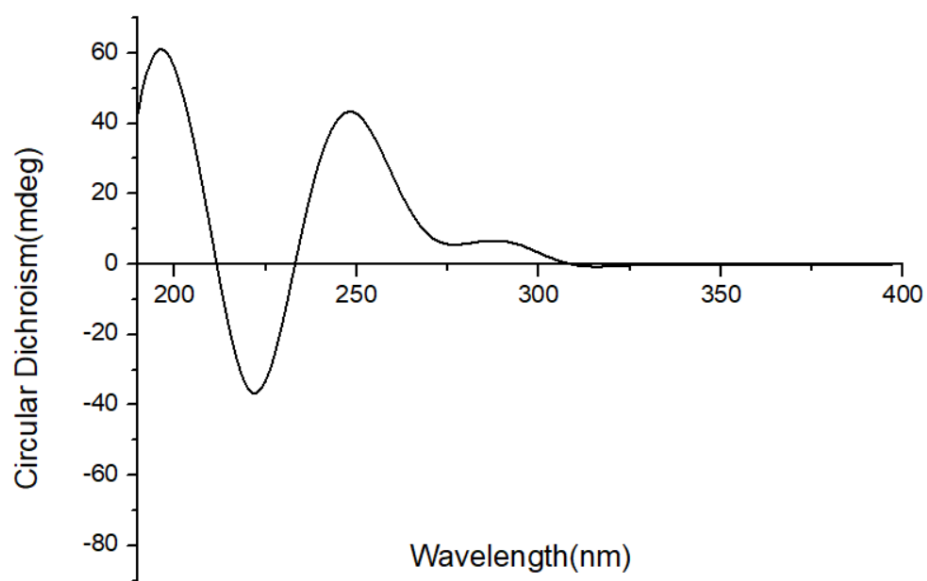


Figure S15. ECD spectrum of compound **1a**

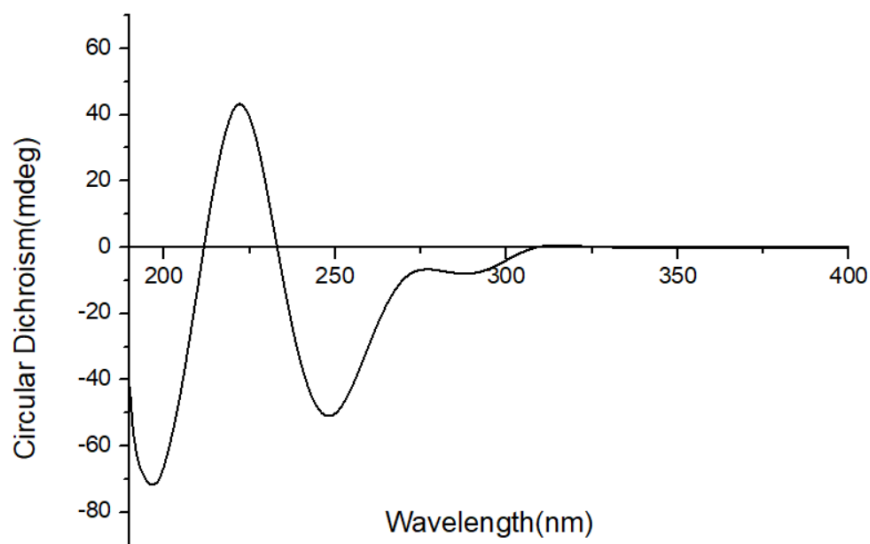


Figure S16. ECD spectrum of compound **1b**

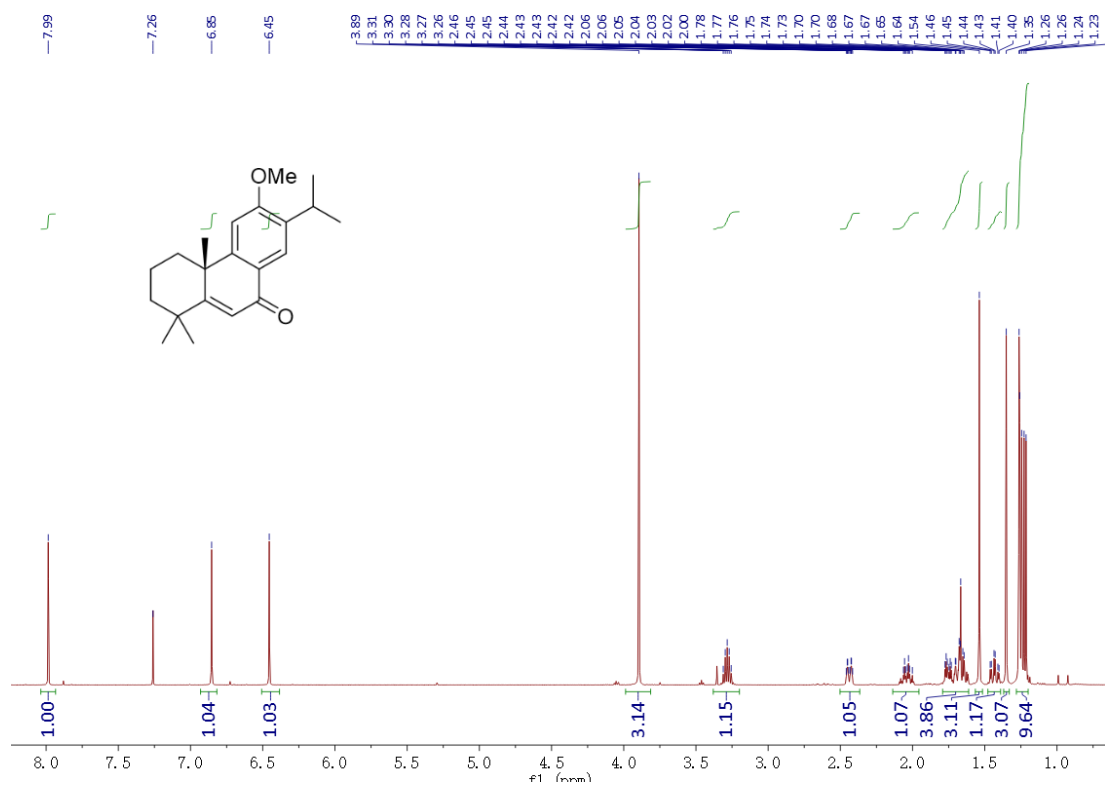


Figure S17. ¹H NMR spectrum of compound 2 in CDCl₃

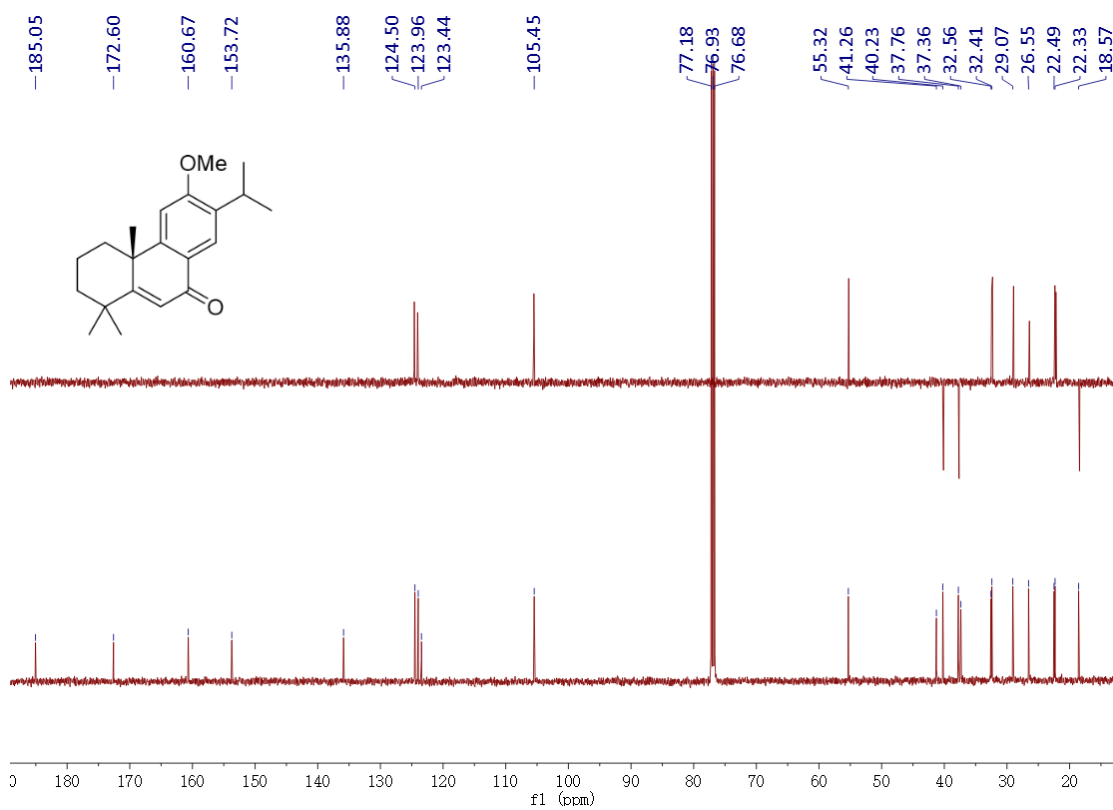


Figure S18. ¹³C NMR spectrum of compound 2 in CDCl₃

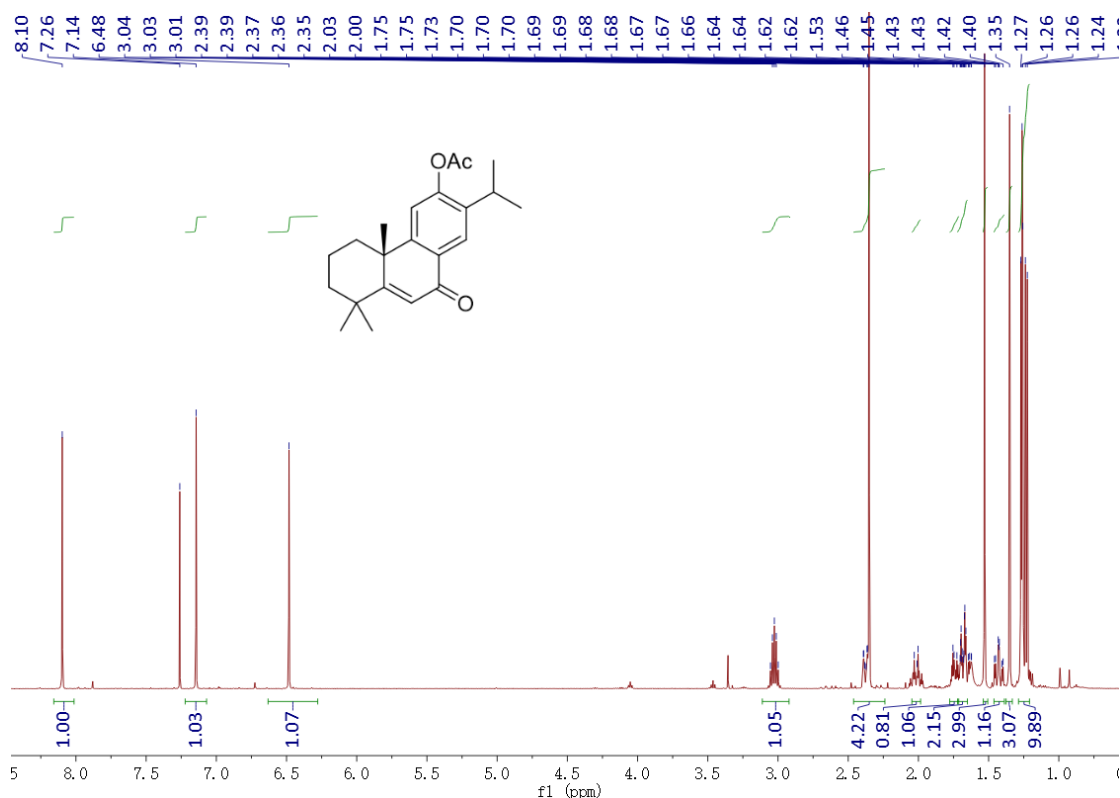


Figure S19. ^1H NMR spectrum of precursor of compound **3** in CDCl_3

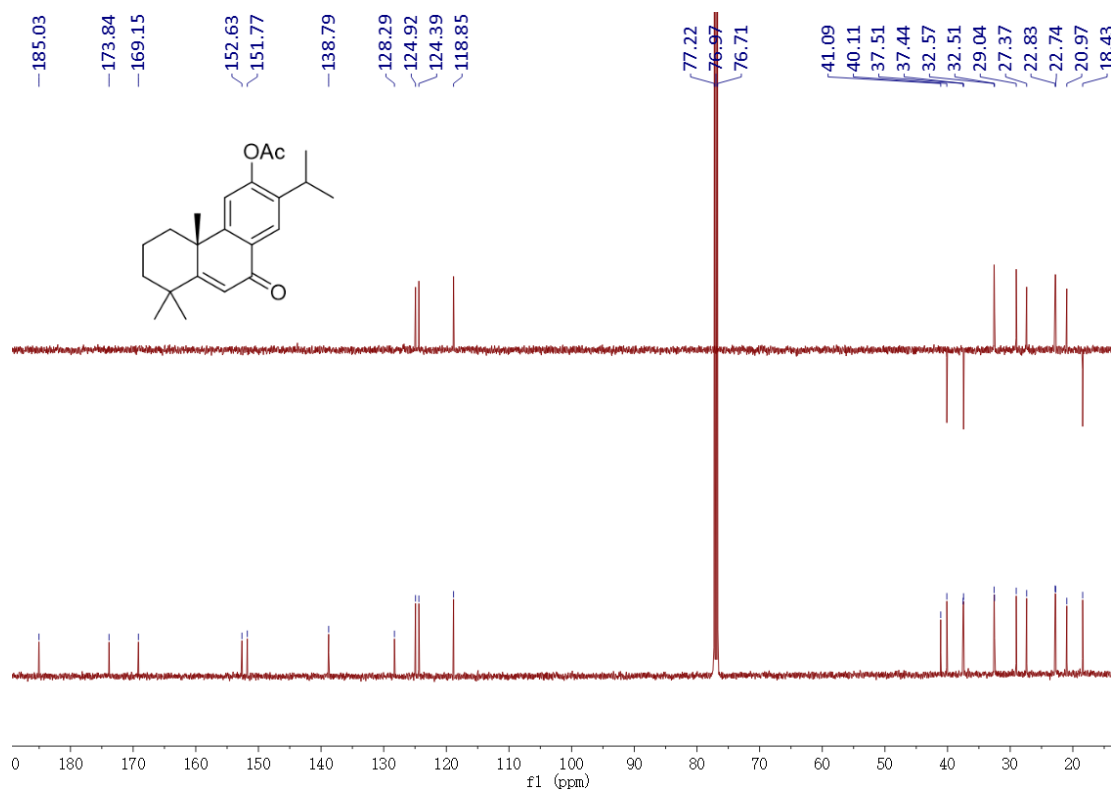


Figure S20. ^{13}C NMR spectrum of precursor of compound **3** in CDCl_3

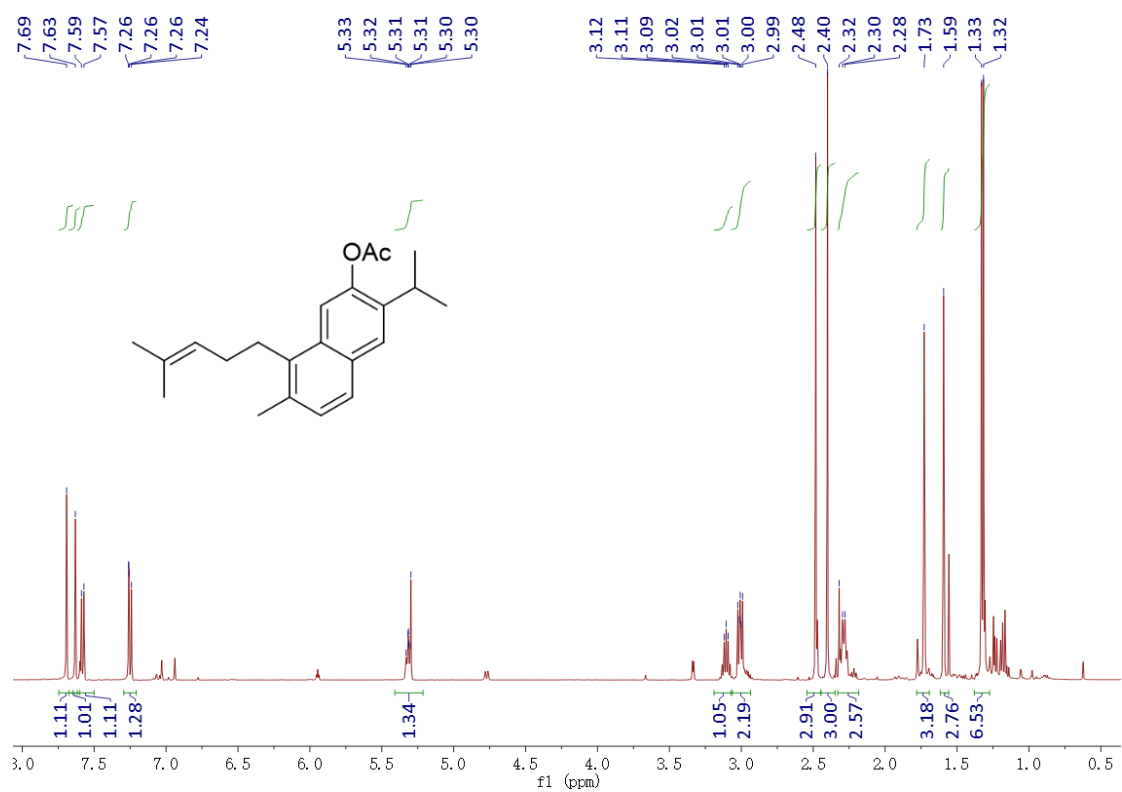


Figure S21. ¹H NMR spectrum of compound **4** in CDCl₃

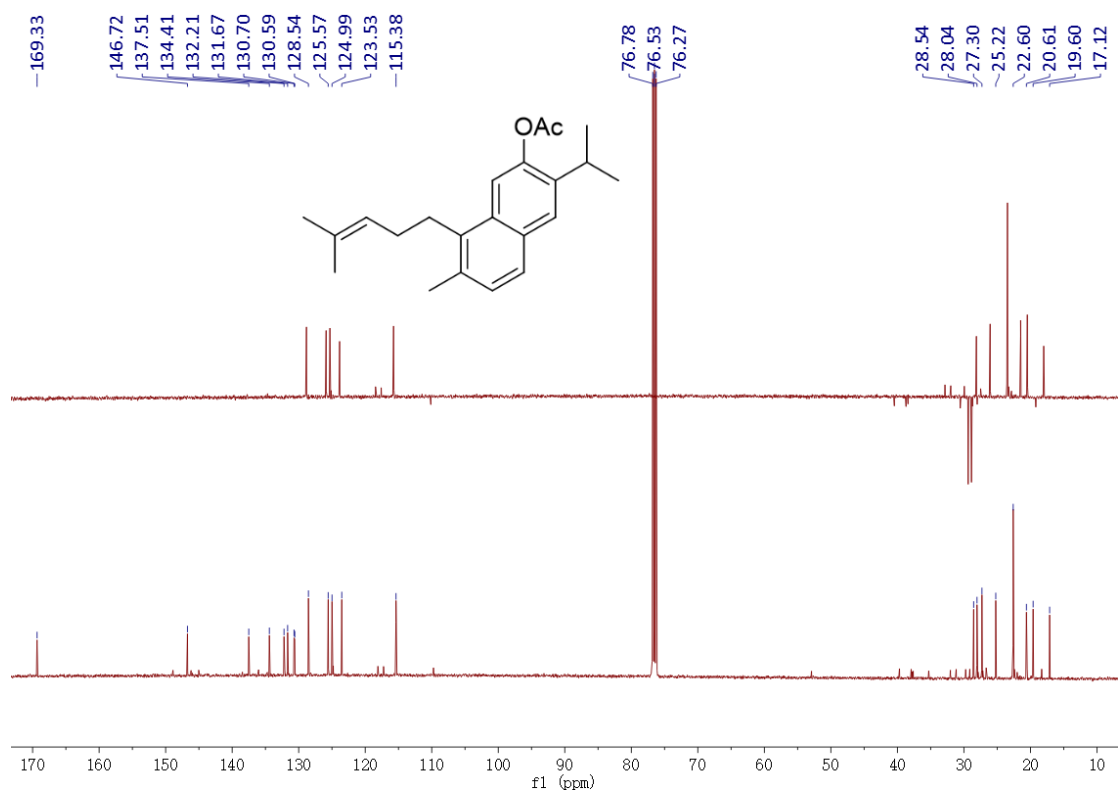


Figure S22. ¹³C NMR spectrum of compound **4** in CDCl₃

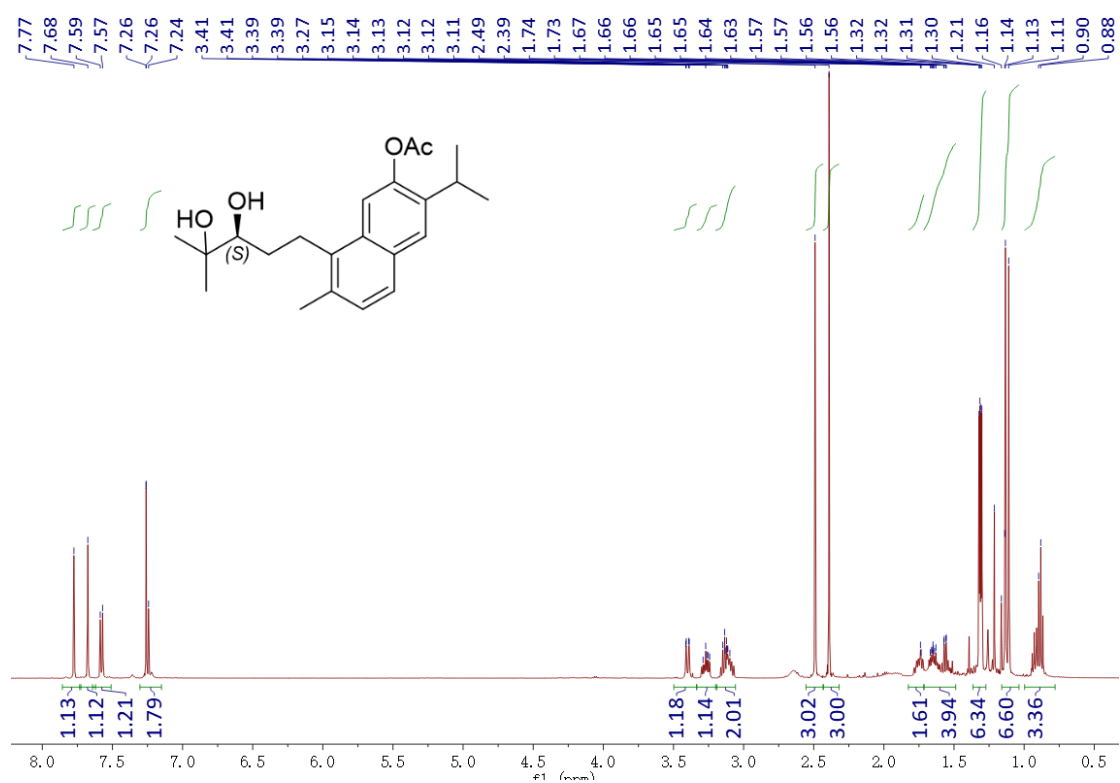


Figure S23. ¹H NMR spectrum of compound **5a** in CDCl₃

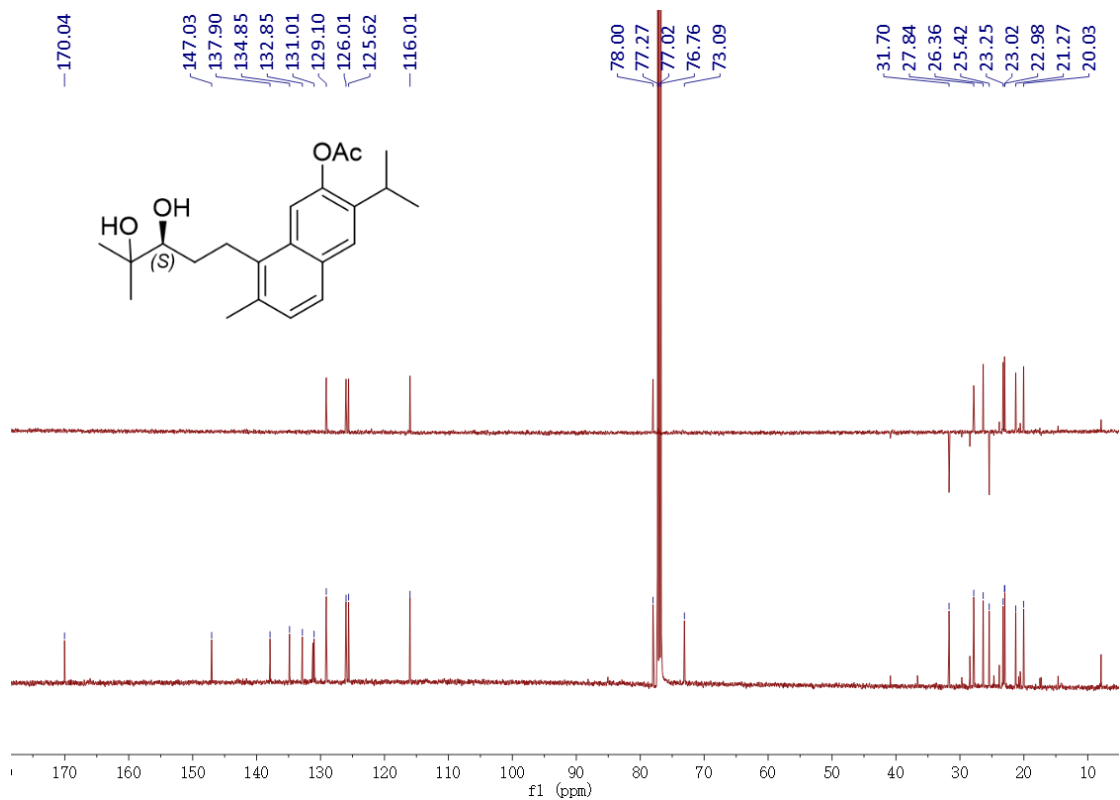


Figure S24. ¹³C NMR spectrum of compound **5a** in CDCl₃

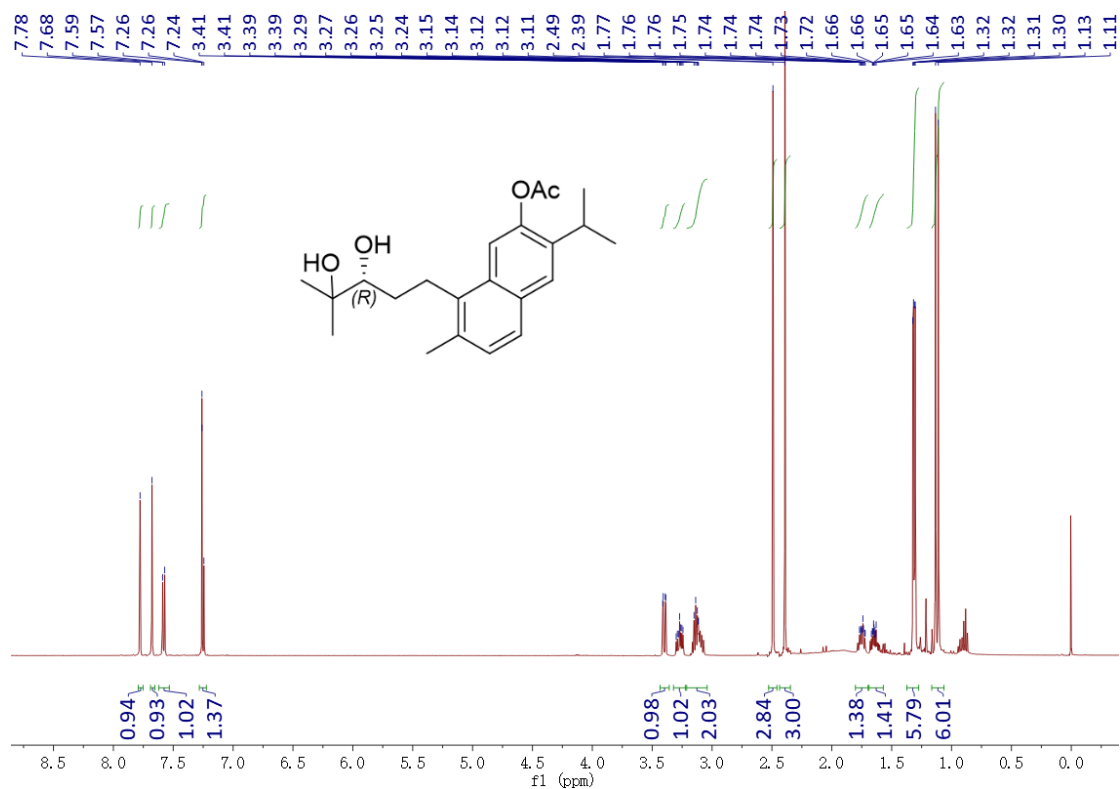


Figure S25. ¹H NMR spectrum of compound **5b** in CDCl₃

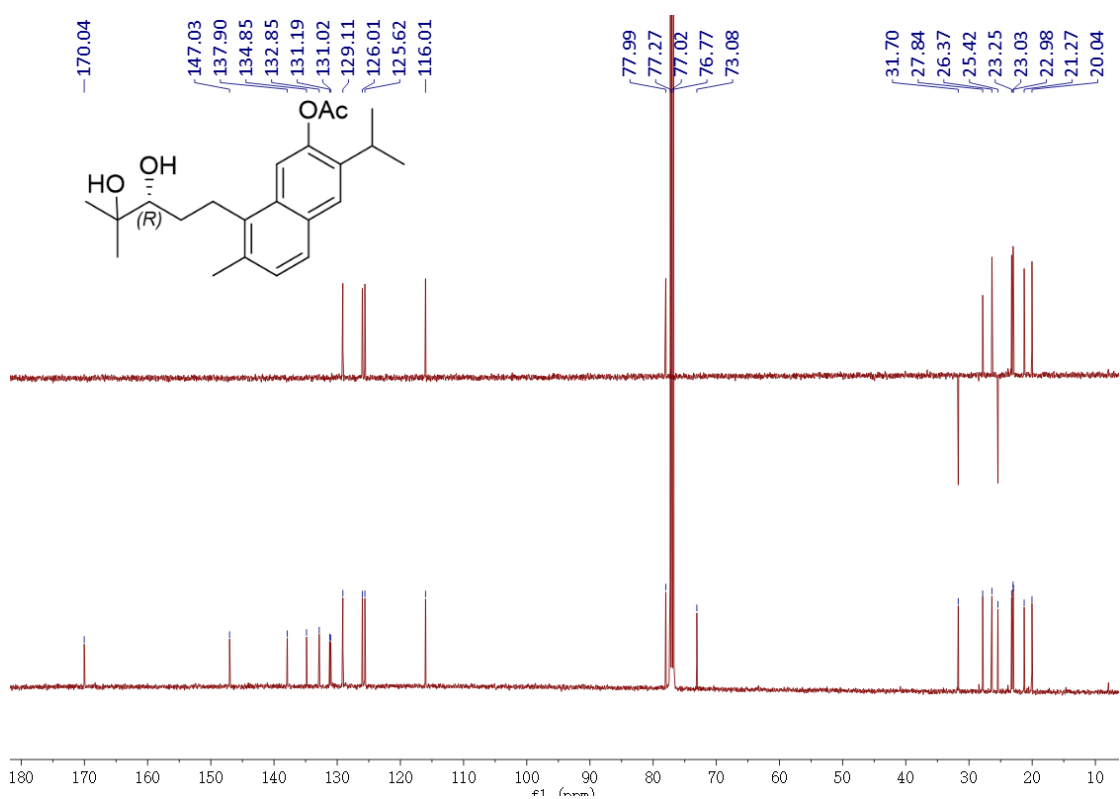


Figure S26. ¹³C NMR spectrum of compound **5b** in CDCl₃

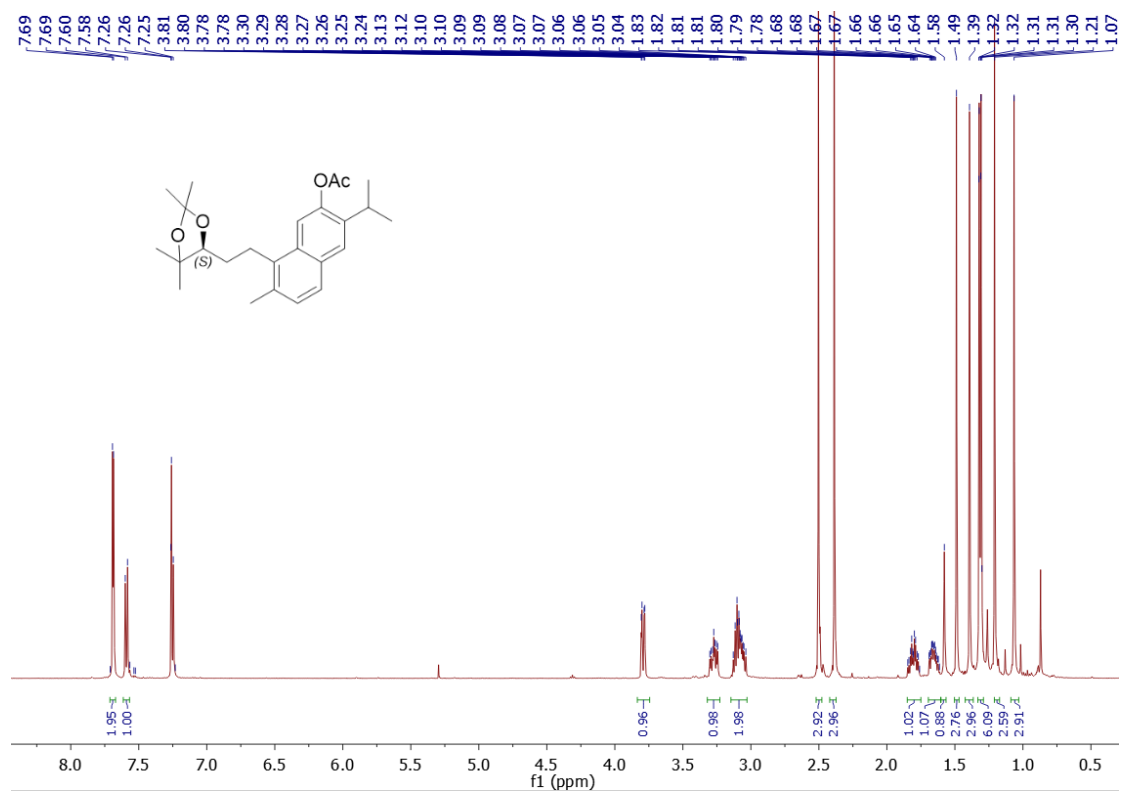


Figure S27. ¹H NMR spectrum of synthetic **6a** in CDCl₃

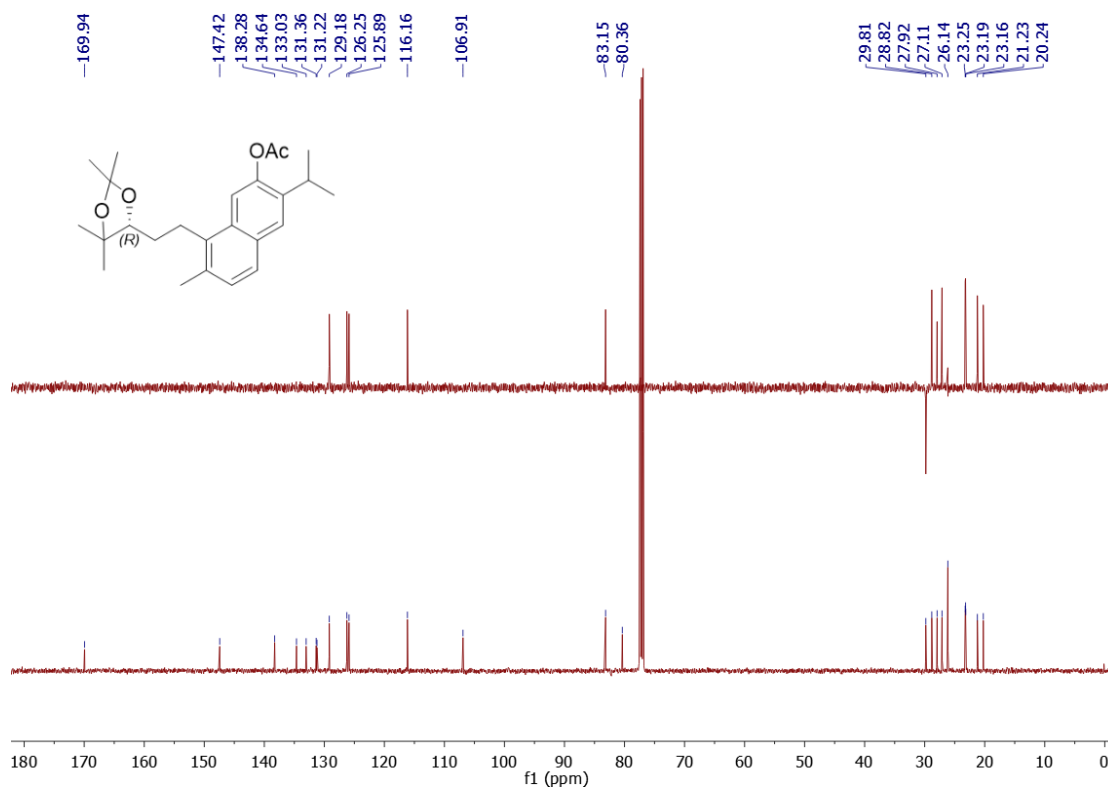


Figure S28. ¹³C NMR spectrum of compound **6a** in CDCl₃

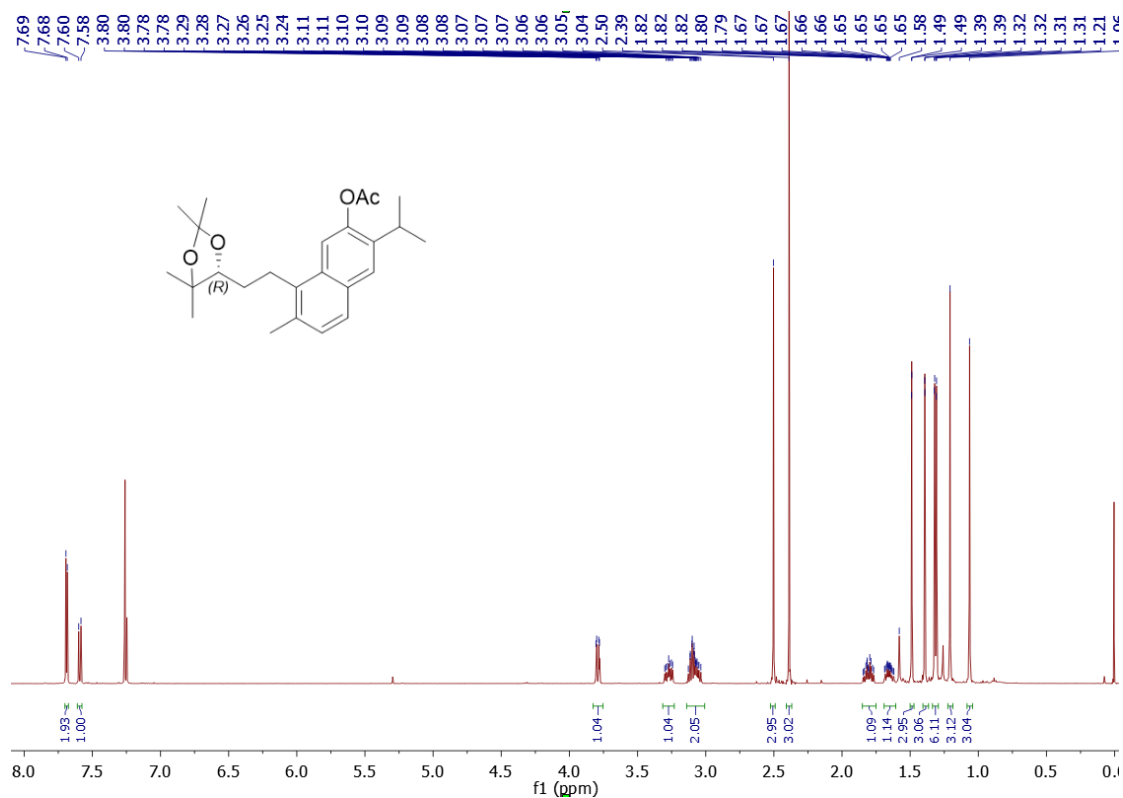


Figure S29. ¹H NMR spectrum of synthetic **6b** in CDCl₃

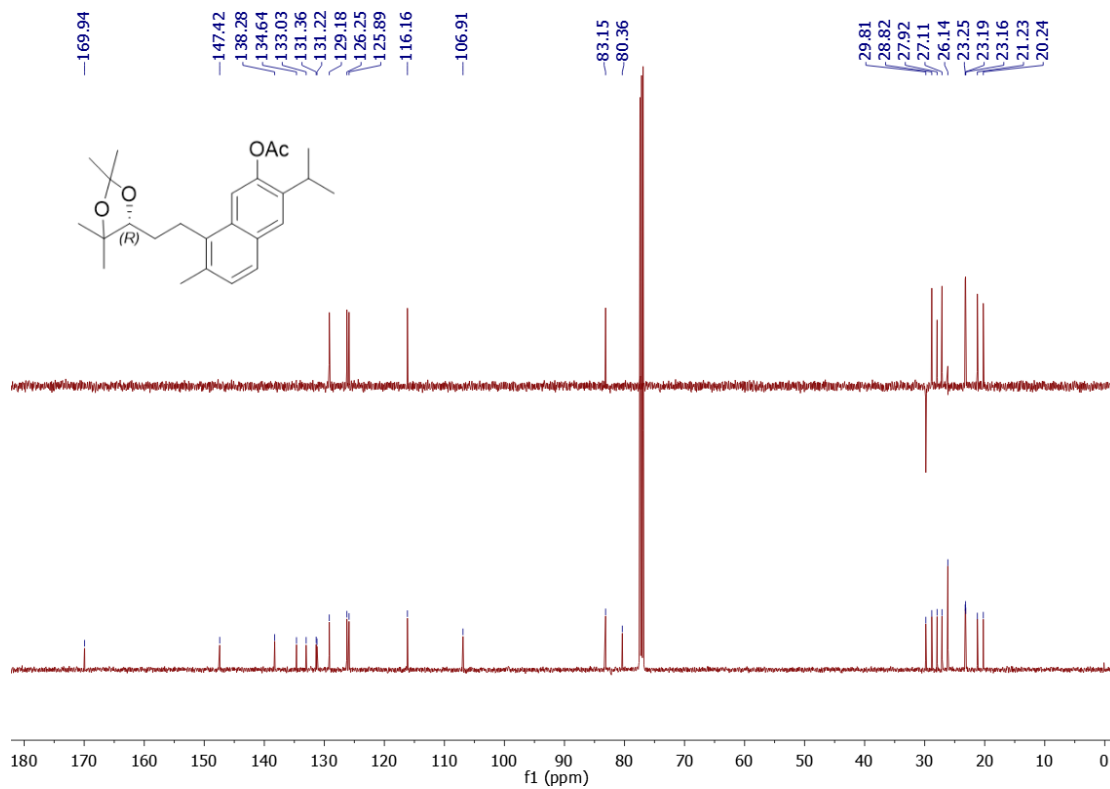


Figure S30. ¹³C NMR spectrum of synthetic **6b** in CDCl₃

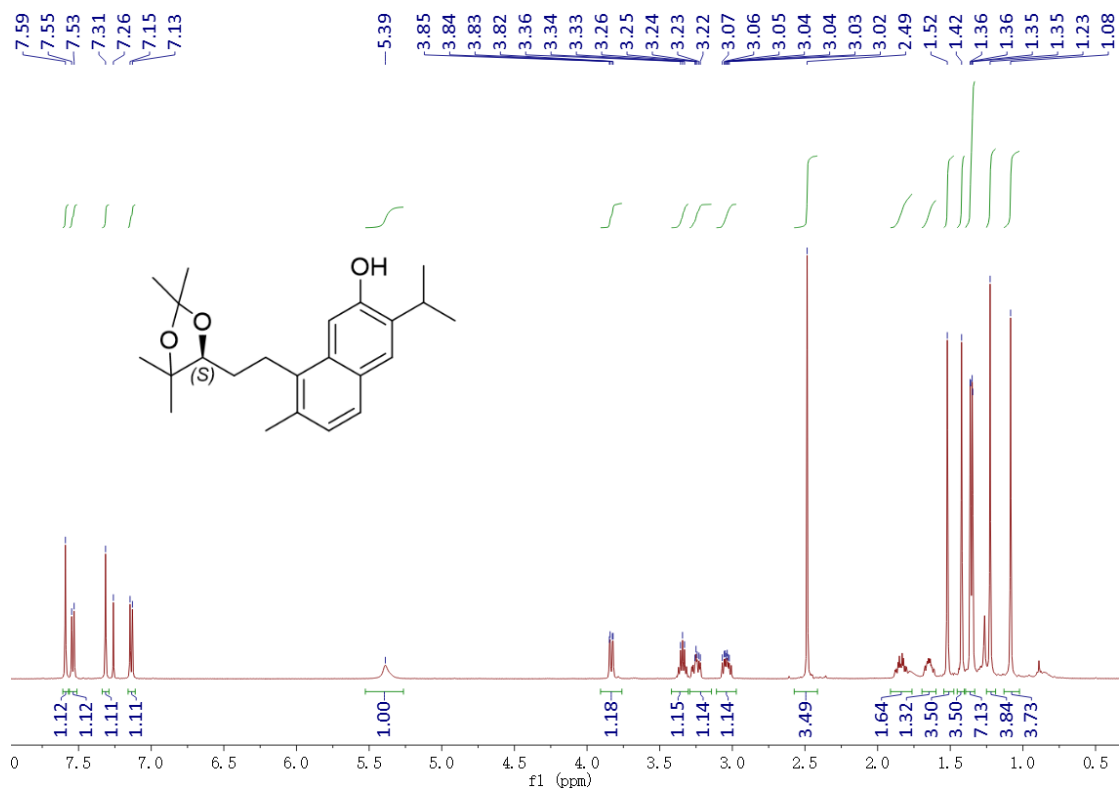


Figure S31. ¹H NMR spectrum of synthetic **7a** in CDCl₃

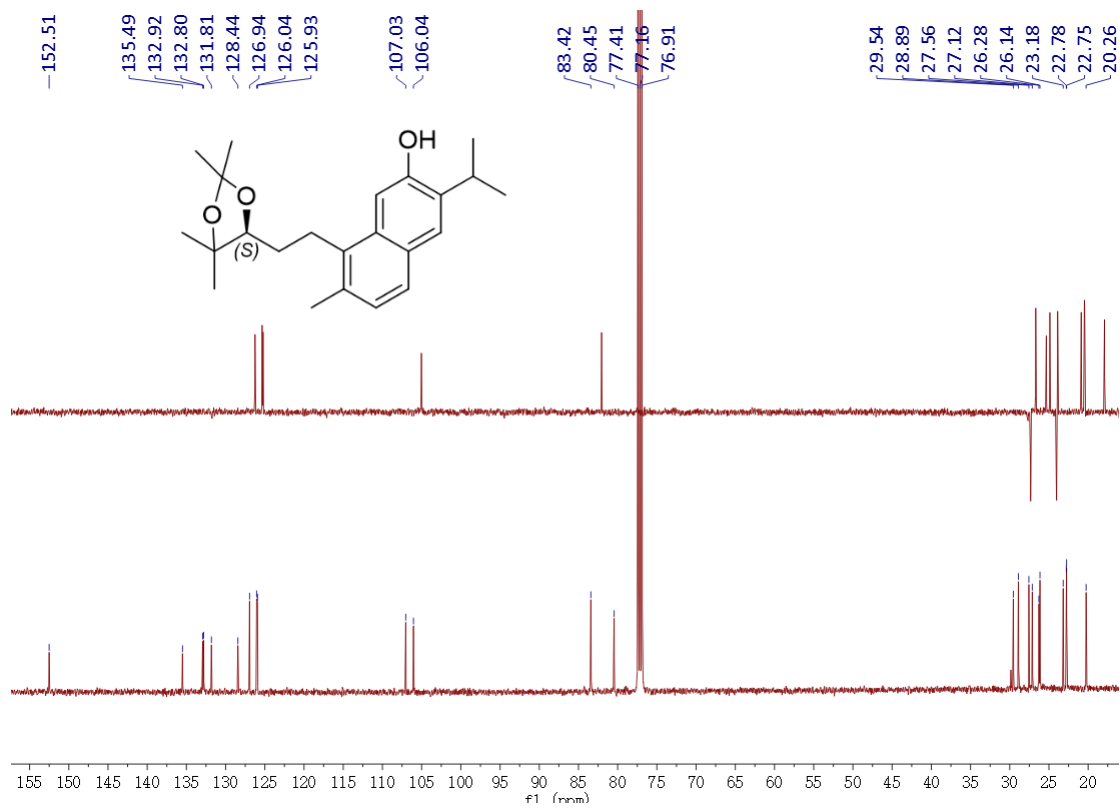


Figure S32. ¹³C NMR spectrum of synthetic **7a** in CDCl₃

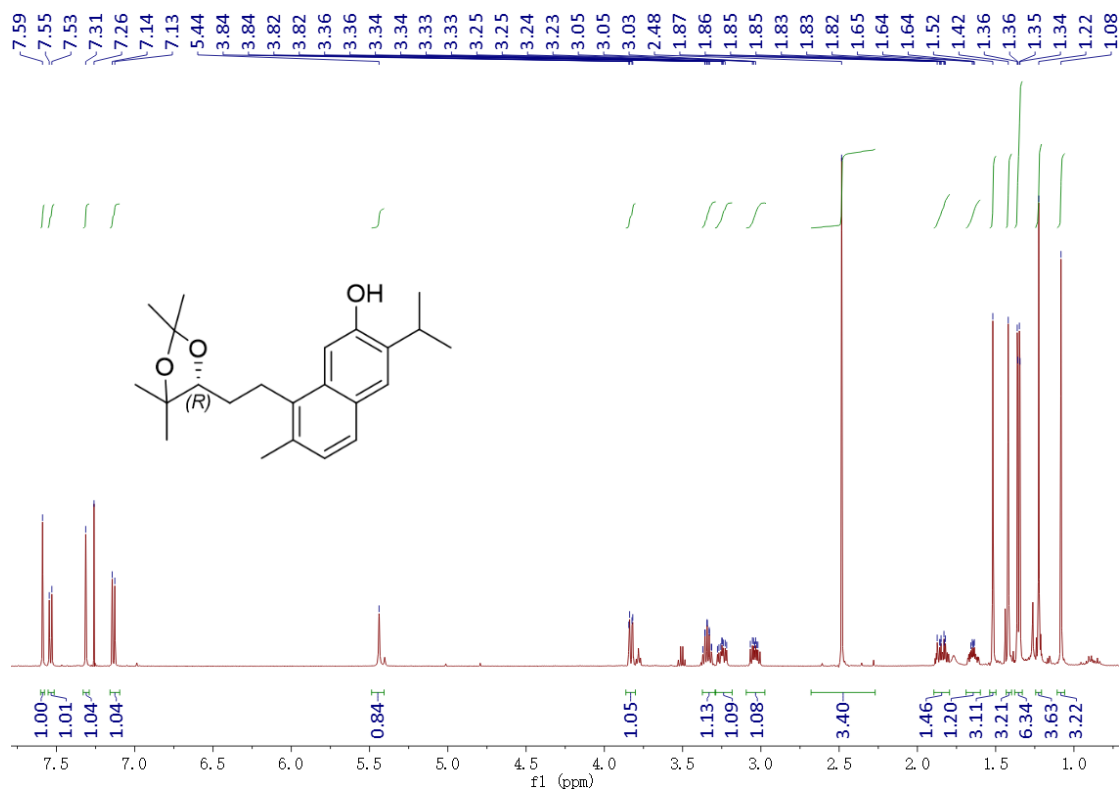


Figure S33. ¹H NMR spectrum of synthetic **7b** in CDCl₃

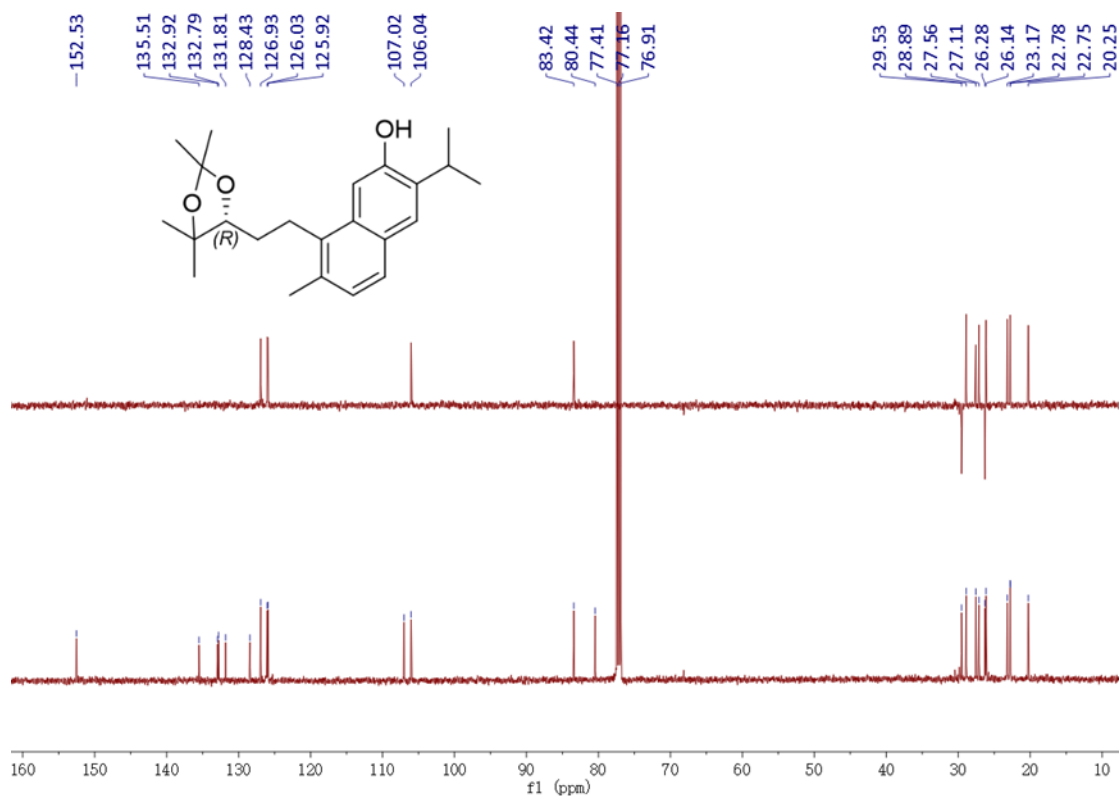


Figure S34. ¹³C NMR spectrum of synthetic **7b** in CDCl₃

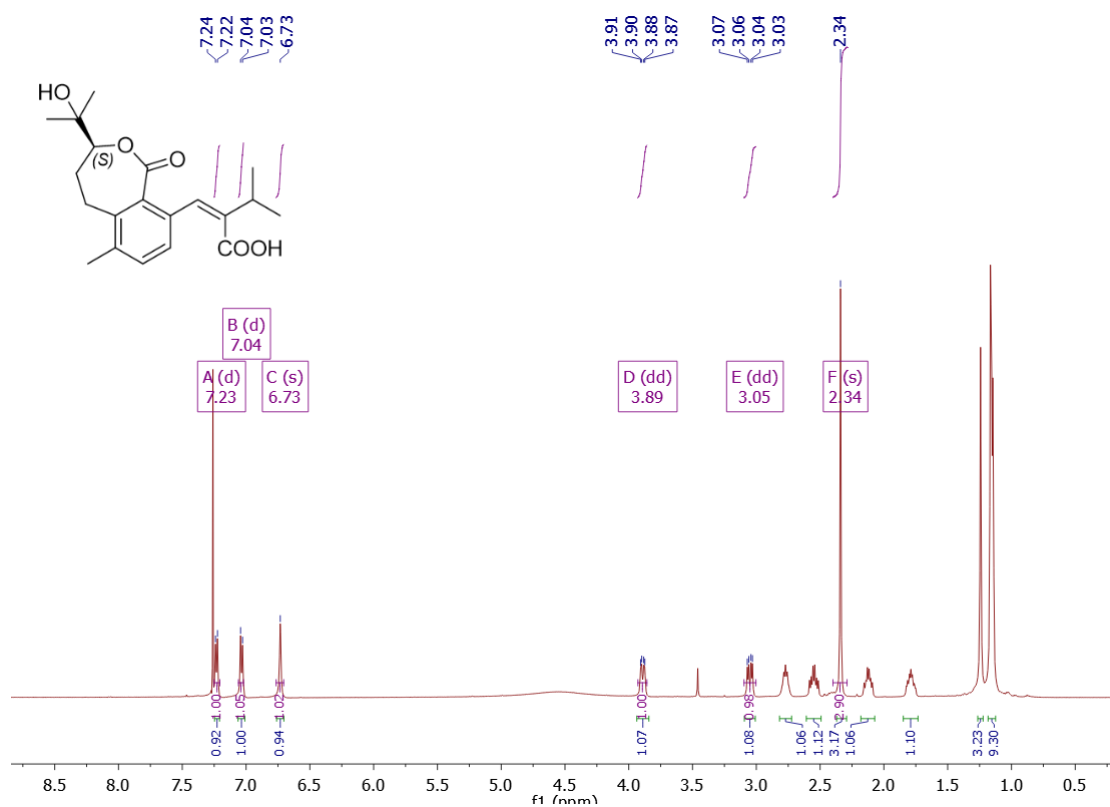


Figure S35. ¹H NMR spectrum of synthetic **1a** in CDCl₃

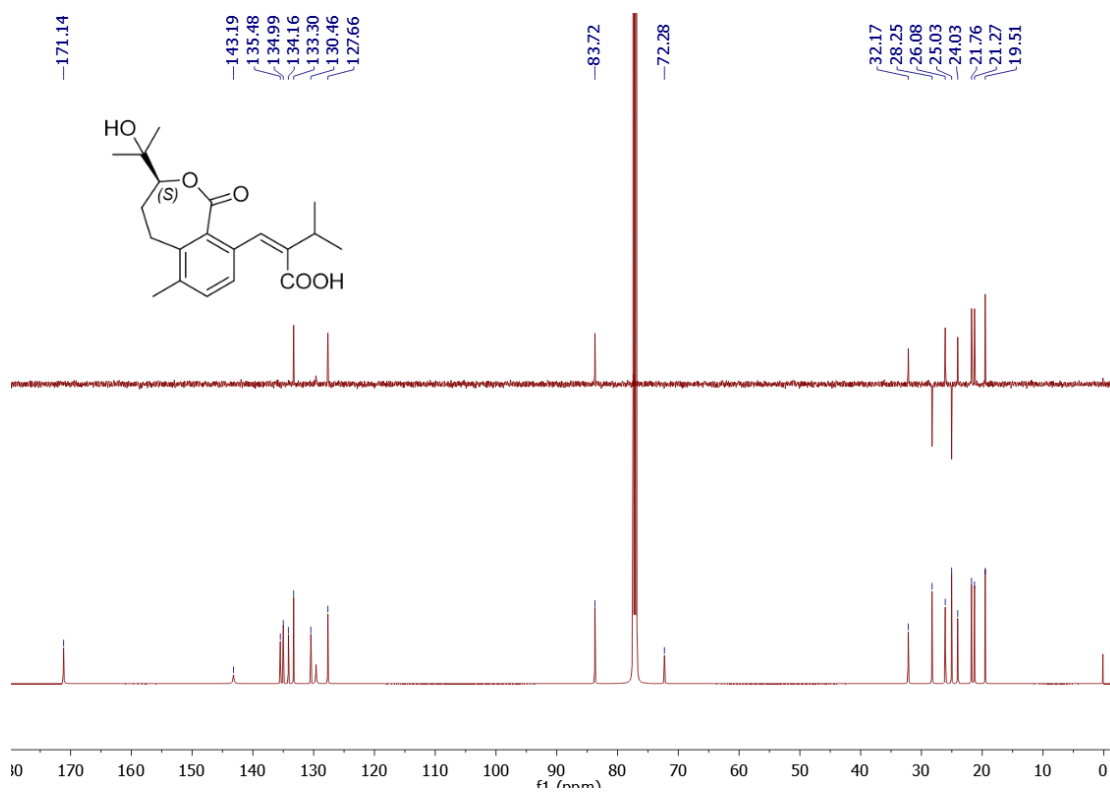


Figure S36. ¹³C NMR spectrum of synthetic **1a** in CDCl₃

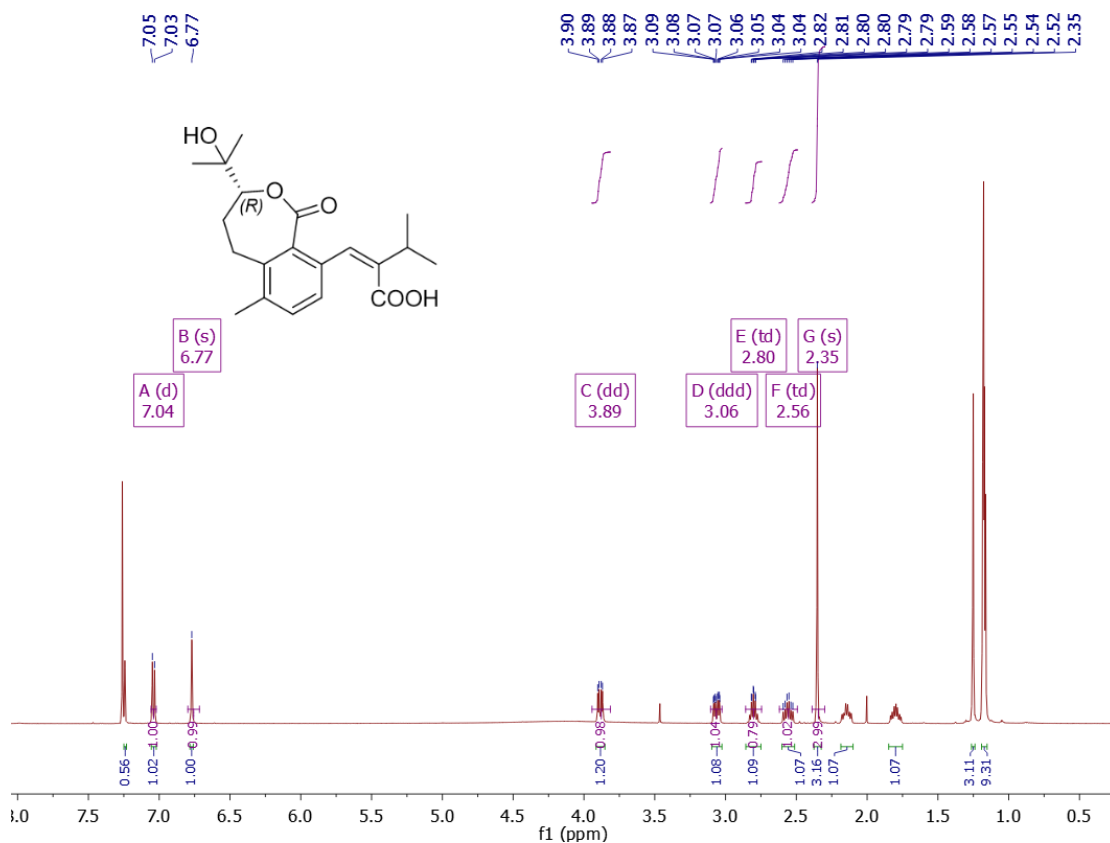


Figure S37. ^1H NMR spectrum of synthetic **1b** in CDCl_3

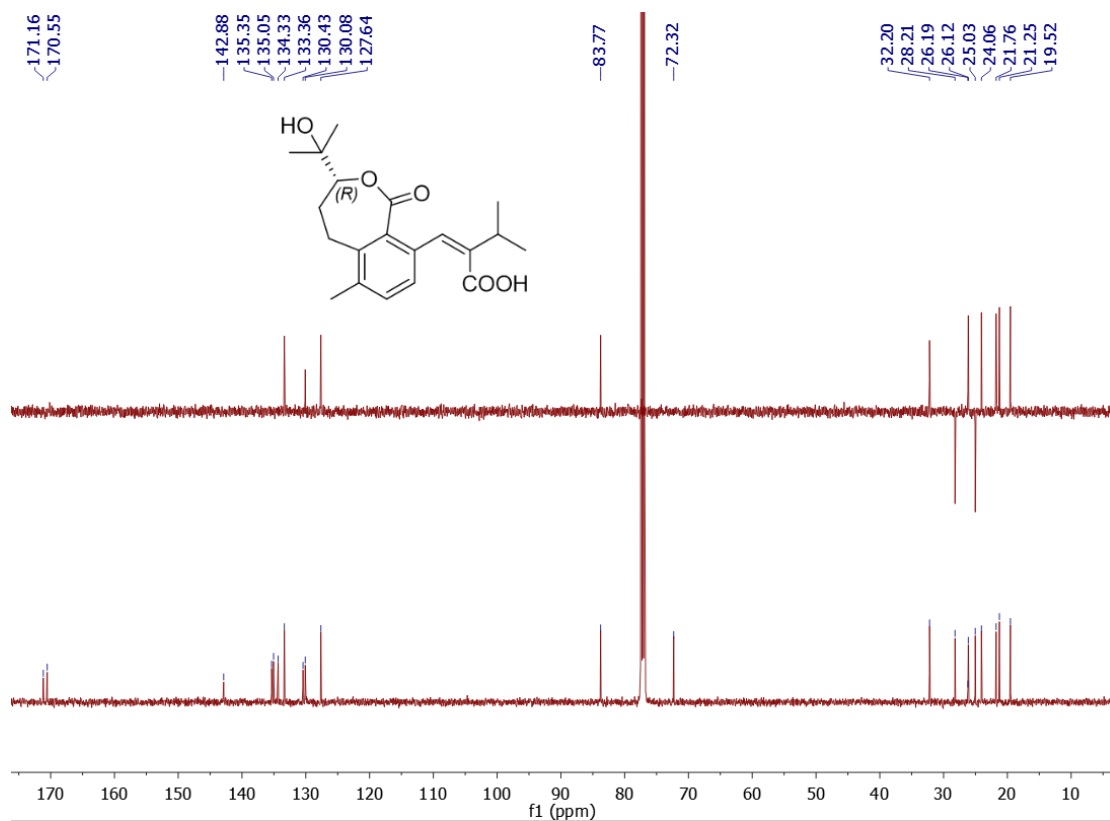


Figure S38. ^{13}C NMR spectrum of synthetic **1b** in CDCl_3